LAWRENCE
LIVERMORE
NATIONAL
LABORATORY

LLNL-JRNL-868053

237Np Fission Spectrum Cumulative Fission Product Yield Measurement Using Godiva IV Critical Assembly

A. S. Tamashiro, J. T. Harke, J. G. Duarte, Y. Mishnayot, S. Burcher, S. W. Padgett, P. Zhao, B. D. Pierson, N. Gharibyan, J. M. Goda, L. R. Greenwood, D. K. Hayes, J. Hutchinson, N. Harward, K. Roberts, G. Slavik, P. Yap-Chiongco, J. Walker, C. J. Palmer

August 8, 2024

Nuclear Data Sheets

Disclaimer

^{237}Np Fission Spectrum Cumulative Fission Product Yield Measurement Using Godiva IV Critical Assembly

A.S. Tamashiro,[1,*] J.T. Harke,[2] J.G. Duarte,[2] Y. Mishnayot,[2] S. Burcher,[2] S.W. Padgett,[2] P. Zhao,[2] B.D. Pierson,[3] N. Gharibyan,[2] J.M. Goda,[4] L.R. Greenwood,[3] D.K. Hayes,[4] J. Hutchinson,[4] N. Harward,[2] K. Roberts,[2] G. Slavik,[2] P. Yap-Chiongco,[2] J. Walker,[4] and C.J. Palmer[1]

[1] *Oregon State University, Corvallis, OR 97331, USA*
[2] *Lawrence Livermore National Laboratory, Livermore, CA 94550, USA*
[3] *Pacific Northwest National Laboratory, Richland, WA 99352, USA*
[4] *Los Alamos National Laboratory, Los Alamos, NM 87545, USA*

(Dated: January 5, 2024; Received xx August 2022; revised received xx September 2022; accepted xx October 2022)

Precise integral measurement of fast neutron-induced fission product yields for various actinides is of high interest for applied nuclear science. The goal of this effort is to improve uncertainties in fission product yield values of ^{237}Np. Fission was induced in a $NpO_2(NO_3)$ target using the Godiva IV critical assembly in burst mode. The irradiated sample was transferred to a high-resolution γ-ray detection setup within 50 minutes. γ-ray list mode data was collected from 50 minutes to 1 week after the irradiation. γ-ray spectroscopy was performed to analyze the time dependent γ-ray yields using an automated peak search algorithm to identify isotopes by their decay γ-ray energy and half-life. The initial activity for each isotope identified was used to calculate their fission product yield.

CONTENTS

* Corresponding author: tamashiro1@llnl.gov

I. INTRODUCTION

The Short-Lived Fission Product Yield (SLFPY) project objective is to provide improved measurements of fission product yields for actinides. The measured fission product yields are needed for various areas of applied and fundamental nuclear science. Data exists for fission product yields on fissioning of ^{235}U [25], ^{238}U [26], and ^{239}Pu [27] with fission spectrum neutrons.

Recently, the Godiva IV critical assembly was utilized to perform a prompt burst irradiation of a sample of ^{237}Np with the goal of measuring fission product yields [28]. A γ spectroscopy-based data analysis procedure has been developed for the prediction of fission product yields that is independent of the actinide sample [29]. These results are part of a series of measurements performed by this research team where ^{235}U, ^{238}U, ^{239}Pu, ^{237}Np, and ^{233}U fission product yields have all been measured using an identical experimental setup and analysis. Some representative results will be presented in this article.

II. BACKGROUND

Fission product yields are used in the prediction of the behavior and performance of engineered systems involving nuclear fission. Measurements of fission product yields have been traditionally performed through radiochemistry, mass spectrometry, and γ-ray spectroscopy, often with mono-energetic neutrons.

To date, the most recent fission product yield evaluation was conducted in 1993 by England and Rider, almost 3 decades ago [30]. There were 653 fission product yield values compiled for ^{237}Np fast neutron-induced fission, 172 of which were measured using radiochemistry. The evaluation compiled publications from 1956 – 1987, making the most recent results three and a half decades old. Although, six of these publications were γ-ray spectroscopy without chemical separation [31–36]. All of these measurements used Ge(Li) or HPGe detectors. One measurement used ^{252}Cf spontaneous fission neutrons, one measurement used a thermal reactor with a 2 mm Cd shield around the sample, and the rest used fission spectrum neutrons. ^{241}Pu fission product yield values from 1987 [35] were included in the ^{237}Np fission product yield evaluation. In total, 43 fission product yield results for 29 isotopes via γ-ray spectroscopy without chemical separation were included in the England and Rider's evaluation. Table I lists these 29 isotopes along with their half-lives and reference fission product yields.

TABLE I. List of isotopes in the England and Rider's evaluation that were measured using γ-ray spectroscopy without chemical separation. Majority of these evaluated ^{237}Np fission product yield values included ^{241}Pu fission product yields (indicated by a checkmark).

Isotope	$\tau_{1/2}$	FPY_{ref} (%) [37]	^{241}Pu [35]
^{85m}Kr	4.480 ± 0.008 h [38]	0.935 ± 0.037	–
^{87}Kr	76.3 ± 0.5 m [39]	1.741 ± 0.049	–
^{87}Br	55.65 ± 0.13 s [39]	1.474 ± 0.162	–
^{88}Kr	2.825 ± 0.019 h [1]	2.096 ± 0.126	–
^{91}Sr	9.65 ± 0.06 h [2]	3.925 ± 0.157	–
^{92}Y	3.54 ± 0.01 h [3]	4.385 ± 0.123	✓
^{92}Sr	2.611 ± 0.017 h [3]	4.371 ± 0.175	–
^{95}Zr	64.032 ± 0.006 d [5]	5.669 ± 0.134	✓
^{97}Zr	16.749 ± 0.008 h [6]	6.111 ± 0.171	✓
^{103}Ru	39.249 ± 0.003 d [8]	5.558 ± 0.156	✓
^{105}Ru	4.439 ± 0.011 h [9]	3.103 ± 0.186	✓
^{130}Sb	39.5 ± 0.8 m [13]	1.169 ± 0.748	✓
^{131}I	8.0252 ± 0.0006 d [14]	3.600 ± 0.072	✓
^{131}Te	25.0 ± 0.1 m [15]	3.031 ± 0.182	✓
^{132}Te	3.204 ± 0.013 d [15]	4.751 ± 0.190	✓
^{133}I	20.83 ± 0.08 h [16]	6.460 ± 4.135	✓
^{133m}Te	55.4 ± 0.4 m [16]	3.587 ± 0.287	✓
^{134}I	52.5 ± 0.2 m [17]	6.953 ± 0.195	✓
^{134}Te	41.8 ± 0.8 m [17]	4.415 ± 0.177	✓
^{135}Xe	9.14 ± 2 h [18]	7.255 ± 0.203	✓
^{135}I	6.58 ± 0.03 h [18]	6.708 ± 0.188	✓
^{137}I	24.5 ± 0.2 s [40]	2.450 ± 0.392	–
^{138}Cs	32.5 ± 0.2 m [41]	6.002 ± 0.240	✓
^{138}Xe	14.14 ± 0.07 m [41]	5.247 ± 0.420	–
^{139}Ba	82.93 ± 0.09 m [19]	5.634 ± 0.225	✓
^{140}La	1.67858 ± 0.00021 d [20]	5.494 ± 0.077	✓
^{140}Ba	12.751 ± 0.004 d [20]	5.488 ± 0.110	✓
^{142}La	91.1 ± 0.5 m [22]	4.794 ± 0.134	✓
^{143}Ce	33.039 ± 0.006 h [23]	4.650 ± 0.186	✓

III. EXPERIMENT

Godiva IV is a critical assembly composed of unreflected highly enriched uranium (HEU) metal fuel [42]. This device was intended to irradiate samples using prompt bursts of fast fission neutrons of around 24 μsec FWHM in duration with a peak neutron flux of around 4×10^{18} neutrons/cm^2/sec [42]. Large neutron fluxes allow shorter irradiation times, minimizing neutron absorption in the subsequent fission products, and assuring larger fission product generation rates. Section III A is reproduced from Reference [27] and is included here for completeness.

A. Data Collection System

The setup consisted of two Broad-Energy Germanium (BEGe) detectors (Canberra, model BE6530), each cou-

FIG. 1. Counting setup.

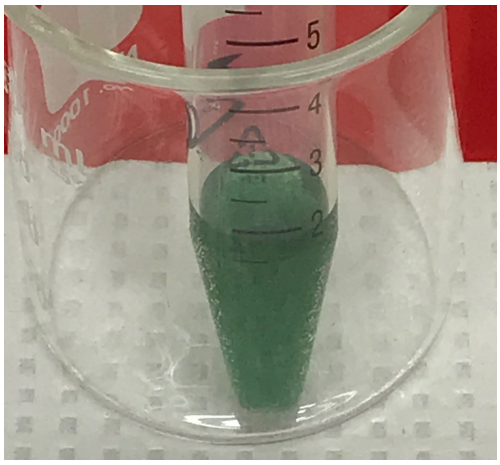

FIG. 2. Solution of neptunium(V) as NpO_2NO_3.

pled to a Lynx data acquisition system. The detectors (labelled as 8815 and 8816) were mounted on 30L liquid nitrogen dewars. The detectors are 180° from each other placed equidistant between them (see Figure 1). The detection volume is surrounded by a lead and copper to reduce background γ rays. A 1/16" thick iron followed by a 1.5 cm Teflon™ disks were placed in front of the detectors. This is to shield the detectors from β-particles and Bremmstrahlung X-rays.

The γ-rays detected by the BEGe spectrometers were stored in list mode format by the Lynx systems (Canberra, Digital Signal Analyzer). Data from each detector were stored in a separate file with each γ-ray interaction recorded by a time stamp and channel number. The timing between detectors was synchronized using a 5 MHz oscillator. such that timing between the two detectors could be used as a filter for coincident events in the future. For data rates of approximately 25 kHz or less the live time fraction of the data acquisition system was high enough to prevent instabilities or errors in data recording with the Lynx data acquisition system.

B. System Calibrations

The BEGe detectors and shielding used for this measurement were exactly the same as those used for previous ^{235}U [25], ^{238}U [26], and ^{239}Pu [27] fission product yield measurements [28]. Radioactive sources of ^{22}Na, ^{60}Co, ^{137}Cs, ^{133}Ba, and ^{152}Eu were placed in the source position and used to determine the energy calibration and detection efficiencies. The neptunium samples were made from a solution of $NpO_2(NO_3)$ (see Figure 2) and dried in quartz ampoules (see Figure 3). The quartz ampoules were flame sealed and leak checked to ensure no fission product gasses escaped during the measurement. The four ^{237}Np samples were counted for short periods (tens of minutes each) on 1/22/2020. From the γ spectra, the masses were determined to be 5.8 mg, 10.7 mg, 20.0 mg, and 42.89 mg for Np1, Np2, Np3, and Np4 respectively. A background measurement was performed for two hours.

C. Irradiation and Measurement

For the irradiation in the central volume of Godiva IV, the witness foils were wrapped together in aluminum foil. These witness foils consisted of small quantities of Cu (100.225 mg), Au (106.210 mg), Co (28.635 mg), Fe (108.108 mg), Ti (81.958 mg), Ni (31.678 mg), and Al (33.368 mg). That packet was placed along with the quartz ampoules in a aluminum sample holder tube into the Godiva glory hole. Figure 3 shows the four samples prior to irradiation.

The four ^{237}Np samples were inserted into Godiva on January 22, 2020 at 10:21 a.m. PST and the burst occurred at 10:57:54 a.m. The radiation monitor (an RMS-III detector) primarily measures gamma dose and exceeded its measurement limit during the burst. 700 R/hr is the highest reading observed before it went over-limit. Two resistance temperature detectors (RTDs) in Godiva IV are used to measure the temperature in the safety block (closest to the center) and in a ring. The safety block's RTD measured the core to be 13.7°C and increased by 137.4°C during the burst. The dose rate from Godiva itself needed to decrease enough for personnel entry to be allowed to retrieve the samples. The samples weren't retrieved until 11:40 a.m. The witness foils and empty quartz ampule were set aside for subsequent packaging and shipment to Pacific Northwest National Laboratory (PNNL). The neptunium samples were packaged together for transport to the counting station at 11:45 a.m. Sample Np2 was mounted on a sample holder and placed in the central location between the BEGe detectors. The detection rate was approximately 30 kHz at 11:48:31 a.m. At 3:05:09 p.m. the data acquisition was stopped, data were saved, then Np1 + Np3 were mounted

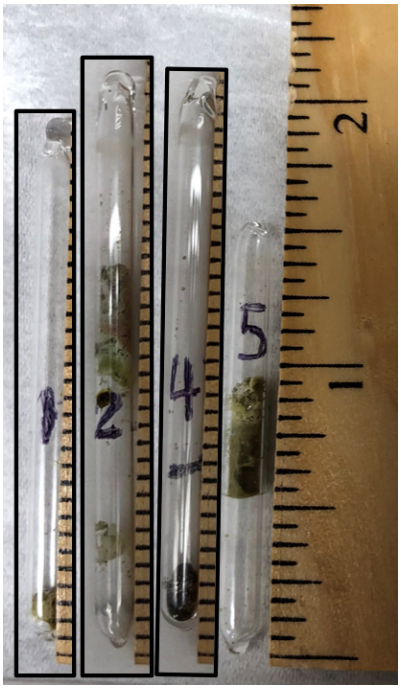

FIG. 3. The $NpO_2(NO_3)/HNO_3$ solutions were delivered into the quartz tubes, then dried under house nitrogen steam and the quartz tubes were flame sealed. The ampoules were labeled 1, 2, 4, and 5, which are samples Np1, Np2, Np3, and Np4 respectively.

and placed in the central position. The second measurement started at 3:31:20 p.m. on January 22, 2020. The detected rate on each system was approximately 20 kHz. The measurement of Np1 and Np3 continued until 09:46 a.m. on January 30, 2020. The room was closed and not accessed except for occasional filling of liquid nitrogen.

D. Witness Foil Analysis

The witness foil pack was irradiated with the neptunium samples and analyzed at PNNL. Table II shows the measured reaction rate for each activated metal. From this measurement, the neutron energy spectrum (see Figure 4) was calculated using the STAYSL PNNL code [43]. The STAYSL analysis estimated 7.3E11 ± 3E10 fission events per gram of the plutonium samples.

IV. DATA ANALYSIS

This section is reproduced from Reference [27] and is included here for completeness. The fission product yield, FPY_i, for isotope i can be calculated directly from the ratio of the number of decay events from isotope i to the total number of fission events in the irradiation experiment. The total number of fission events N_f is generated assuming a known reference fission product yield,

TABLE II. Witness foil reactions and measured sample activation values, corrected to the burst irradiation time.

Sample	Mass (mg)	Reaction	Isotope	Reaction Rate $[\sigma\phi]$ ($s^{-1}atom^{-1}$)
Cu	100.225	^{63}Cu(n,γ)	^{64}Cu	3.6E-12 ± 1E-13
		^{63}Cu(n,α)	^{60}Co	8.4E-14 ± 3E-15
Au	106.210	^{197}Au(n,γ)	^{198}Au	3.56E-11 ± 7E-13
		^{197}Au(n,2n)	^{196}Au	5.6E-13 ± 1E-14
Co	28.635	^{59}Co(n,γ)	^{60}Co	2.10E-12 ± 4E-14
Fe	108.108	^{58}Fe(n,γ)	^{59}Fe	7.3E-13 ± 4E-14
		^{54}Fe(n,p)	^{54}Mn	1.24E-11 ± 2E-13
		^{56}Fe(n,p)	^{56}Mn	1.70E-13 ± 3E-15
		^{54}Fe(n,α)	^{51}Cr	1.19E-13 ± 9E-15
Ti	81.958	^{46}Ti(n,p)	^{46}Sc	1.75E-12 ± 4E-14
		^{47}Ti(n,p)	^{47}Sc	2.98E-12 ± 6E-14
		^{48}Ti(n,p)	^{48}Sc	4.9E-14 ± 1E-15
Ni	31.678	^{58}Ni(n,p)	^{58}Co	1.58E-11 ± 3E-13
		^{60}Ni(n,p)	^{60}Co	1E-13 ± 1E-14
Al	33.368	^{27}Al(n,α)	^{24}Na	3.36E-13 ± 7E-15

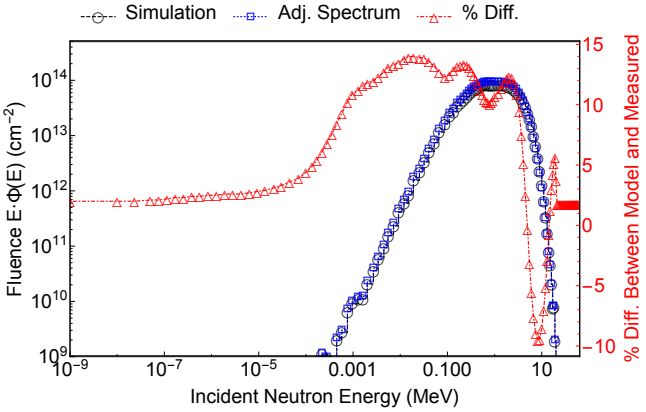

FIG. 4. A plot of the MCNP simulated and adjusted neutron fluence spectrum for Godiva IV during the ^{237}Np pulsed irradiation.

FPY_{ref}:

$$N_f = \frac{A_{0,ref}\tau_{1/2,ref}}{\ln(2)FPY_{ref}\epsilon_{\gamma ref}I_{ref}R_{ref}}. \quad (1)$$

The measured fission yield for isotope i can then be written in terms of the reference isotope:

$$\frac{FPY_i}{FPY_{ref}} = \left(\frac{A_{0,i}}{A_{0,ref}}\right)\left[\frac{\tau_{1/2,i}/\epsilon_{\gamma,i}I_iR_i}{\tau_{1/2,ref}/\epsilon_{\gamma,ref}I_{ref}R_{ref}}\right]. \quad (2)$$

Where should be used, A_0 is the initial activity of the induced radioactive fission product, $\tau_{1/2}$ is the half-life of the specific isotope, ϵ_γ is the absolute detector efficiency,

I is the self attenuation of the γ ray through the target, and R is the branching ratio of the γ ray observed. The activities, half-life, and efficiencies are measured in the experiment, while the other parameters are from ENDF-VIII.0 [37]. The reference fission product used to estimate the total number of fission events is ^{140}Ba (^{99}Mo and ^{140}Ba are common standards for fission product yield measurements [44]).

A. Detector Efficiency – ϵ_γ

TABLE III. Eckert & Ziegler calibration sources used for detector characterization.

Source	$\tau_{1/2}$	Activity (kBq)	Date
^{60}Co	1925.28 ± 0.14 d [45]	44 ± 1	8/1/2019
^{137}Cs	30.08 ± 0.09 y [40]	41 ± 4	8/1/2019
^{22}Na	2.6018 ± 0.0022 y [46]	42 ± 1	8/1/2019
^{133}Ba	312.20 ± 0.20 d [47]	42 ± 1	8/1/2019
^{152}Eu	10.551 ± 0.011 y [16]	44 ± 1	8/1/2019

Table III lists the calibration sources used. This data is used for energy calibration and detector efficiency fits. The equation used to fit the detector efficiency is the following:

$$\epsilon_\gamma = P_0 E^{-P_1} + P_2 - P_3 e^{-P_4 E} \tag{3}$$

where E is energy in MeV. The parameters 0–4 were extracted from the efficiency fit (see Table IV and Figures 5 and 6). The uncertainty was calculated using the following ROOT generated covariance matrices:

	P_0	P_1	P_2	P_3	P_4
P_0	1.4E-9	-3.8E-7	-1.4E-9	-1.3E-7	-1.6E-6
P_1	-3.8E-7	1.1E-4	3.6E-7	3.6E-5	3.5E-4
P_2	-1.4E-9	3.6E-7	1.4E-9	1.2E-7	1.6E-6
P_3	-1.3E-7	3.6E-5	1.2E-7	1.3E-5	1.3E-4
P_4	-1.6E-6	3.5E-4	1.6E-6	1.3E-4	5.6E-3

	P_0	P_1	P_2	P_3	P_4
P_0	1.0E-9	-3.3E-7	-1.0E-9	-9.5E-8	-1.7E-6
P_1	-3.3E-7	1.1E-4	3.1E-7	3.3E-5	4.5E-4
P_2	-1.0E-9	3.1E-7	1.0E-9	8.9E-8	1.6E-6
P_3	-9.5E-8	3.3E-5	8.9E-8	1.0E-5	1.4E-4
P_4	-1.7E-6	4.5E-4	1.6E-6	1.4E-4	6.6E-3

for detector 8815 and 8816 respectively.

B. Self-Attenuation – I

The self attenuation factor accounts for the γ rays attenuating effect through the ^{237}Np samples, and is represented by the following:

$$I = \frac{I_{raw}}{C} = e^{-\frac{\mu}{\rho} x \rho} \tag{4}$$

TABLE IV. Efficiency curve parameters.

P_i	Detector 8815	Detector 8816
[0]	$2.18 \times 10^{-3} \pm 4 \times 10^{-5}$	$1.80 \times 10^{-3} \pm 3 \times 10^{-5}$
[1]	1.08 ± 0.01	1.09 ± 0.01
[2]	$1.41 \times 10^{-3} \pm 4 \times 10^{-5}$	$1.23 \times 10^{-3} \pm 3 \times 10^{-5}$
[3]	0.210 ± 0.004	0.178 ± 0.003
[4]	26.63 ± 0.07	26.44 ± 0.08

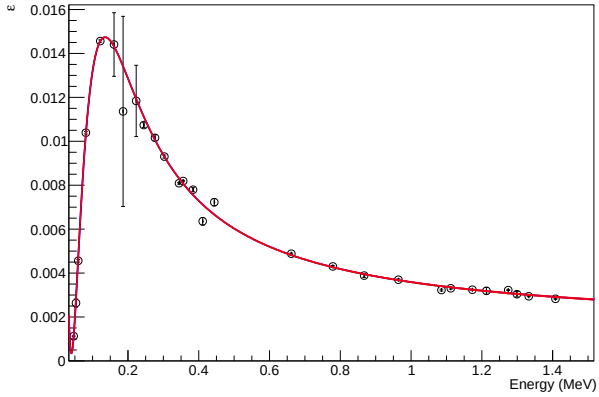

FIG. 5. The detection efficiency of detector 8815 was measured for different calibration sources.

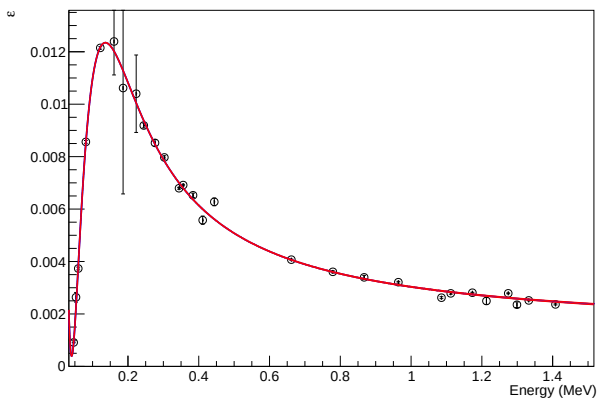

FIG. 6. The detection efficiency of detector 8816 was measured for different calibration sources.

where I_{raw} is the unnormalized self attenuation factor, C is the corrected counts without attenuation, μ/ρ is the mass attenuation for ^{237}Np (provided by NIST XCOM [48]), x is the mean free path, and ρ is the density of ^{237}Np (20.25 g/cm^3 [49]). Figures 7, 8, 9, and 10 are corrected counts of ^{237}Np γ rays listed in Table V and fitted with Equation 4. The normalized counts resulted in Np2 mass to be 12.0 ± 0.6 mg and 11.9 ± 0.6 mg for detectors 8815 and 8816 respectively. The gravimetrically measured Np2 mass was 10.7 mg. The Np2 sample mass difference is caused by a position offset of the sample

TABLE V. ^{237}Np γ-rays used to determine the self attenuation factor.

E_γ (keV)	R_γ	Np1+Np3	Np2
117.7	$1.70 \times 10^{-3} \pm 0.04 \times 10^{-3}$	–	✓
134.3	$7.2 \times 10^{-4} \pm 0.3 \times 10^{-4}$	✓	✓
143.2	$4.16 \times 10^{-3} \pm 0.11 \times 10^{-3}$	–	✓
151.4	$2.44 \times 10^{-3} \pm 0.03 \times 10^{-3}$	✓	–
194.7	$1.82 \times 10^{-3} \pm 0.05 \times 10^{-3}$	✓	–
212.3	$1.52 \times 10^{-3} \pm 0.03 \times 10^{-3}$	✓	–
214.0	$3.57 \times 10^{-4} \pm 0.03 \times 10^{-4}$	✓	–

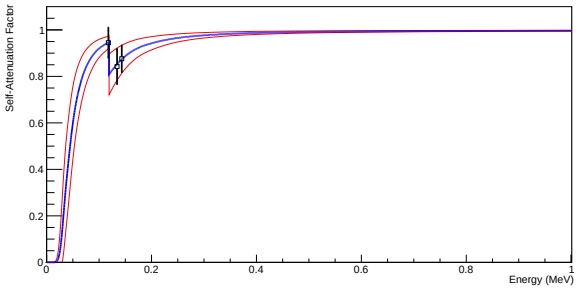

FIG. 7. Np2 self attenuation measured with detector 8815 where x = 2E-3 ± 1E-3 cm.

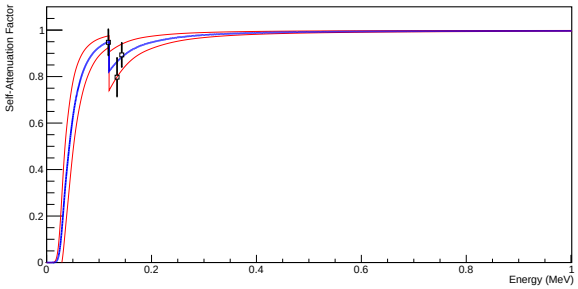

FIG. 8. Np2 self attenuation measured with detector 8816 where 2E-3 ± 1E-3 cm.

compared to the position of the calibration sources. The normalized counts resulted in large Np1 + Np3 mass to be 25.9±0.7 mg and 26.1±0.7 mg for detectors 8815 and 8816 respectively. The gravimetrically measured Np1 and Np3 masses were 5.8 mg and 20.0 mg respectively, which summed to 25.8 mg. The Np1 + Np3 mass difference is caused by a position offset of the sample compared to the position of the calibration sources.

C. Total Fission – N_f

The total number of fission events used in this analysis was calculated with Equation 1. The reference fission product is ^{140}Ba, specifically the 537.3 keV γ-ray from Np1 + Np3. Table VII lists the parameters used to determine the total number of fission events. All fission product yield values in this paper will use the weighted mean of the total number of fission events between the two detectors. Np2's total number of fission events is based on Np1 + Np3's result for ^{142}La 894.9 keV γ-ray.

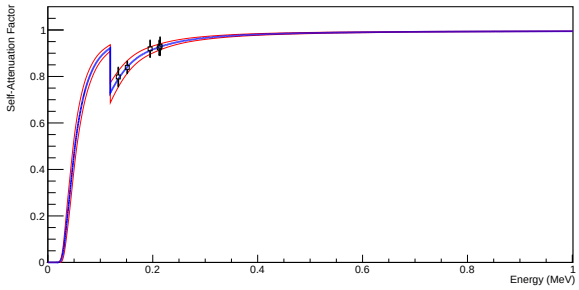

FIG. 9. Np1 + Np3 self attenuation measured with detector 8815 where x = 3.4E-3 ± 6E-4 cm.

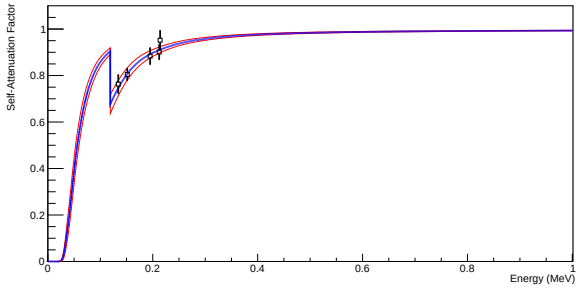

FIG. 10. Np1 + Np3 self attenuation measured with detector 8816 where x = 4.2E-3 ± 6E-4 cm.

TABLE VI. Parameters used to determine Np1 + Np3's total number of fission events.

Parameter		
Isotope	^{140}Ba	
$\tau_{1/2}$ (d)	12.751 ± 0.004 [20]	
FPY (%)	5.488 ± 0.110 [37]	
E_γ (keV)	537.261 ± 0.009 [20]	
R_γ (%)	24.39 ± 0.22 [20]	
Detector	8815	8816
A_0 (Bq)	$8.53 \times 10^{-1} \pm 2 \times 10^{-3}$	$7.20 \times 10^{-1} \pm 2 \times 10^{-3}$
ϵ_γ	$5.68 \times 10^{-3} \pm 1 \times 10^{-5}$	$4.79 \times 10^{-3} \pm 1 \times 10^{-5}$
I_γ	$9.88 \times 10^{-1} \pm 2 \times 10^{-3}$	$9.86 \times 10^{-1} \pm 2 \times 10^{-3}$
N_f	$1.81 \times 10^{10} \pm 4 \times 10^{8}$	$1.81 \times 10^{10} \pm 4 \times 10^{8}$
$\overline{N_f}$	$1.81 \times 10^{10} \pm 4 \times 10^{8}$	

D. γ-Ray Analysis

The γ ray peaks are analyzed using a code written in ROOT [50]. By defining unique energy intervals for each

TABLE VII. Parameters used to determine Np2's total number of fission events.

Parameter		
Isotope	^{142}La	
$\tau_{1/2}$ (hrs)	1.518 ± 0.008 [22]	
FPY (%)	5.5 ± 0.2 (Np1 + Np3 result)	
E_γ (keV)	894.9 ± 0.4 [22]	
R_γ (%)	8.34 ± 0.17 [22]	
Detector	8815	8816
A_0 (Bq)	$1.62 \times 10^1 \pm 1 \times 10^{-1}$	$1.41 \times 10^1 \pm 1 \times 10^{-1}$
ϵ_γ	$3.87 \times 10^{-3} \pm 2 \times 10^{-5}$	$3.27 \times 10^{-3} \pm 2 \times 10^{-5}$
I_γ	$9.96 \times 10^{-1} \pm 2 \times 10^{-3}$	$9.96 \times 10^{-1} \pm 2 \times 10^{-3}$
N_f	$7.2 \times 10^9 \pm 3 \times 10^8$	$7.5 \times 10^9 \pm 3 \times 10^8$
$\overline{N_f}$	$7.3 \times 10^9 \pm 3 \times 10^8$	

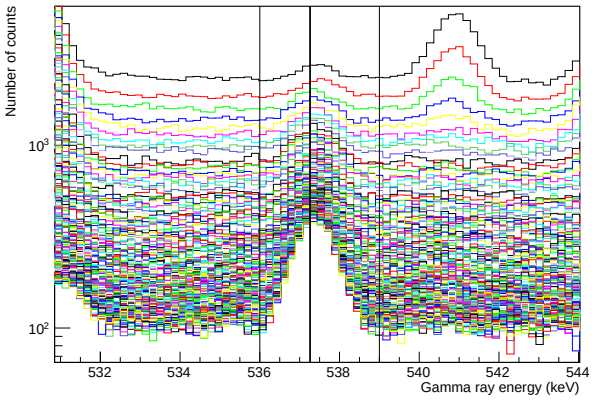

FIG. 11. ^{140}Ba γ-ray cascade plot for the 537.3 keV γ ray. For more details, please refer to the text.

peak, we isolate the peaks in the spectrum so they can be analyzed independently. These intervals are determined visually using cascade plots as illustrated in Figure 11 for the case of a γ-ray peak at 537.3 keV associated with the fission product ^{140}Ba. Each color represents a different time bin and as time progresses the overall counts decrease. In this example, the energy interval is set to [536 keV, 539 keV]. The interval chosen attempts to include information of the background and photo-peak.

As the time binned data is acquired, the live and raw time are used for the dead time correction by multiplying the counts for an energy bin with the ratio of raw time divided by live time. The energy bin channel number is converted into energy deposited by multiplying by the ratio of total energy range to the total number of energy bins. In this case, the energy range is [0,2600 keV] and there are 16384 energy channel bins. The time binned data are histograms of counts vs. energy for each time bin. When the time and energy intervals are chosen, a Gaussian fit function with a linear background is used to

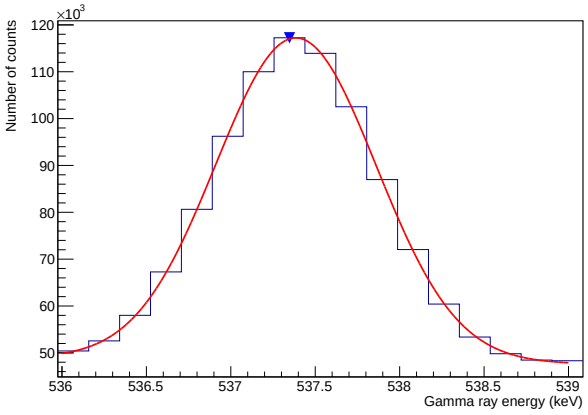

FIG. 12. ^{140}Ba master sum plot fit for the 537.3 keV γ ray

fit the histogram for each time:

$$F(E) = N \exp\left[-\frac{(E-\mu)^2}{2\sigma^2}\right] + mE + y, \tag{5}$$

where N is the amplitude of the peak, μ is the energy of the peak, σ is the resolution of the detector, m is the slope of the background, y is the y-intercept of the background, and E is energy. This technique is used when there is a background continuum present [51]. Before the code fits every time slice, a master fit is produced to provide the centroid of the γ-ray peak [see Figure 12]. The histogram for the master fit is the produced by summing the data over all the time bins in the chosen time interval for each channel.

The linear background is subtracted out and the integral S is the net counts in each respective time bin.

$$\begin{aligned} S &= \int \left(N \exp\left[-\frac{(E-\mu)^2}{2\sigma^2}\right] + mE + y \right) dx \\ &\quad - \int (mE + y)\, dx \\ &= \int \left(N \exp\left[-\frac{(E-\mu)^2}{2\sigma^2}\right] \right) dx. \end{aligned} \tag{6}$$

E. Decay Curve Fitting Routine – $\tau_{1/2}$, A_0

Net counts and half-life data are used to fit a decay curve that is extrapolated to time zero. The data for this curve consists of the counts integrated over each peak (using the energy interval established previously) in each time bin . To secure a proper decay curve, the half life and time increments were fixed. The only parameter to change would be the initial count rate. Provided is the fit function:

$$\begin{aligned} N(t) = &\left(\frac{A_0 \tau_{1/2}}{\ln(2)}\right)\left(\exp\left(-\frac{\ln(2)}{\tau_{1/2}}t\right)\right. \\ &\left. - \exp\left(-\frac{\ln(2)}{\tau_{1/2}}(t+\Delta t)\right)\right), \end{aligned} \tag{7}$$

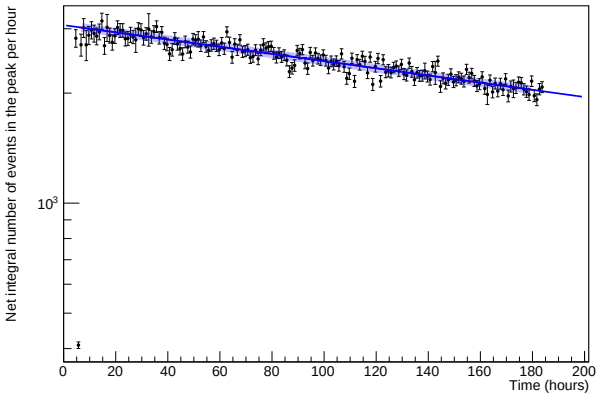

FIG. 13. ^{140}Ba γ-ray half-life plot for the 537.3 keV γ ray

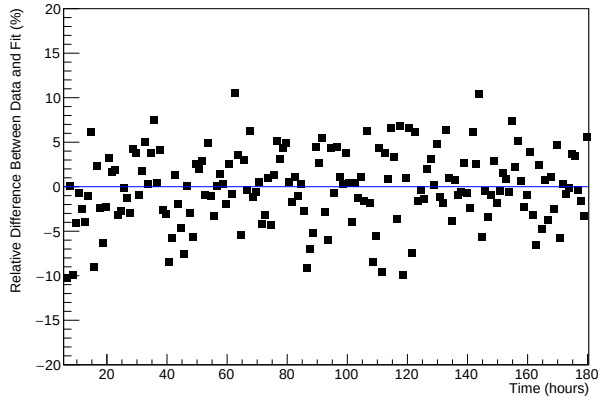

FIG. 14. ^{140}Ba γ-ray residual plot for the 537.3 keV γ ray

where $N(t)$ is the counts of γ rays, A_0 is the initial count rate of γ rays, $\tau_{1/2}$ is half life, Δt is time step, and t is time. This equation is derived from the integral of the count rate over a time bin.

Figure 13 shows the number of events in the peak per hour bin, where the blue line is the fit function and the thicker line indicates the time interval used in the fitting. The black points are the net counts with error for each time bin.

Figure 14 shows the residuals plot from the fitting in Figure 13. The residual plot is another criteria used to help determine an energy and time interval for the γ ray analysis. A time interval is iterated until residuals are less than a user-defined value of 20%. The goal is to include as much fitting points as possible, while minimizing the relative differences in the residual plot.

V. RESULTS

For Np1 + Np3, 20 isotopes were analyzed using 64 γ-rays, resulting in 64 cumulative fission product yield results (see Table VIII). For Np2, 17 isotopes were analyzed using 37 γ-rays, resulting in 37 cumulative fission product yield results (see Table IX). 10 isotopes from Np2 overlapped with results from Np1 + Np3. These were ^{88}Kr, ^{91}Sr, ^{92}Sr, ^{93}Y, ^{105}Ru, ^{127}Sn, ^{131}I, ^{135}I, ^{142}La, and ^{143}Ce. In total, 27 different isotopes were analyzed from this experiment. Since only a single decay curve fit was used, all results are cumulative fission product yields.

TABLE VIII: Np1 + Np3 cumulative fission product yield results from detectors 8815 and 8816. Values were combined by an uncertainty weighted mean. Reference values are from ENDF/B-VIII.0 [37]. ^{99}Mo reference fission product yield for 739.5 keV γ-ray was used to determine the total number of fission events.

Isotope	E_γ (keV)	FPY_{8815} (%)	ΔFPY_{8815} (%)	FPY_{8816} (%)	ΔFPY_{8816} (%)	$\overline{FPY}$ (%)	$\Delta\overline{FPY}$ (%)	FPY_{ref} (%)	ΔFPY_{ref} (%)
^{88}Kr	834.830	1.973	0.110	1.949	0.109	1.961	0.077	2.096	0.126
^{88}Kr	1518.390	1.723	0.124	1.879	0.134	1.794	0.091	2.096	0.126
^{88}Kr	1529.770	1.804	0.104	1.755	0.102	1.779	0.073	2.096	0.126
^{88}Kr	2029.840	1.762	0.109	1.739	0.110	1.751	0.077	2.096	0.126
^{88}Kr	2195.842	1.660	0.094	1.661	0.096	1.661	0.067	2.096	0.126
^{88}Kr	2392.110	1.646	0.093	1.635	0.094	1.640	0.066	2.096	0.126
^{91}Sr	749.800	3.970	0.167	3.958	0.167	3.964	0.118	3.925	0.157
^{92}Sr	1383.930	3.554	0.246	3.491	0.242	3.522	0.172	4.371	0.175
^{93}Y	266.900	4.728	0.693	4.737	0.695	4.732	0.491	5.116	3.275
^{93}Y	947.100	4.885	0.710	5.071	0.736	4.975	0.511	5.116	3.275
^{93}Y	1917.800	4.124	0.569	4.223	0.584	4.172	0.408	5.116	3.275
^{95}Zr	756.725	5.495	0.138	5.592	0.142	5.542	0.099	5.669	0.113
^{97}Zr	254.170	7.191	0.564	8.029	0.657	7.546	0.428	6.111	0.171
^{97}Zr	355.400	6.530	0.342	6.283	0.331	6.402	0.238	6.111	0.171
^{97}Zr	507.640	5.838	0.261	5.775	0.258	5.806	0.184	6.111	0.171
^{97}Zr	602.370	6.849	0.413	6.062	0.372	6.414	0.276	6.111	0.171
^{97}Zr	703.760	5.496	0.347	5.466	0.355	5.481	0.248	6.111	0.171

^{97}Zr	1147.970	6.411	0.300	6.310	0.296	6.360	0.211	6.111	0.171
^{97}Zr	1362.680	5.829	0.641	5.775	0.655	5.803	0.458	6.111	0.171
^{97}Zr	1750.240	5.134	0.503	4.962	0.489	5.046	0.351	6.111	0.171
^{99}Mo	739.500	6.625	0.203	6.507	0.200	6.565	0.142	6.118	0.245
^{99}Mo	777.921	6.385	0.202	6.459	0.207	6.421	0.145	6.118	0.245
^{103}Ru	497.085	5.866	0.166	5.723	0.162	5.793	0.116	5.558	0.156
^{105}Ru	469.370	3.241	0.131	3.270	0.132	3.256	0.093	3.103	0.186
^{105}Ru	499.300	3.788	0.544	3.550	0.511	3.662	0.373	3.103	0.186
^{105}Ru	676.360	3.482	0.143	3.408	0.140	3.444	0.100	3.103	0.186
^{105}Ru	724.300	3.367	0.092	3.326	0.092	3.346	0.065	3.103	0.186
^{127}Sn	1114.300	0.221	0.048	0.224	0.048	0.223	0.034	0.258	0.082
^{129}Sb	544.700	1.168	0.087	1.149	0.086	1.158	0.061	1.759	0.405
^{129}Sb	633.700	0.730	0.092	0.714	0.095	0.722	0.066	1.759	0.405
^{129}Sb	812.800	1.476	0.078	1.454	0.077	1.465	0.055	1.759	0.405
^{131m}Te	793.750	1.040	0.037	1.087	0.038	1.063	0.026	0.683	0.075
^{131m}Te	852.210	0.800	0.031	0.786	0.031	0.793	0.022	0.683	0.075
^{131m}Te	1125.460	0.819	0.037	0.793	0.037	0.806	0.026	0.683	0.075
^{131m}Te	1206.600	0.792	0.030	0.775	0.030	0.784	0.021	0.683	0.075
^{131}I	364.489	3.934	0.105	3.904	0.105	3.919	0.074	3.600	0.072
^{131}I	636.989	4.124	0.121	4.173	0.123	4.148	0.086	3.600	0.072
^{133}I	529.872	6.790	0.269	6.799	0.269	6.794	0.190	6.460	4.135
^{133}I	1298.223	7.376	0.311	7.263	0.309	7.319	0.219	6.460	4.135
^{135}I	220.502	7.472	0.337	7.135	0.340	7.305	0.239	6.708	0.188
^{135}I	836.804	6.670	0.283	6.594	0.280	6.632	0.199	6.708	0.188
^{135}I	1038.760	6.617	0.277	6.565	0.276	6.591	0.196	6.708	0.188
^{135}I	1131.511	6.594	0.270	6.564	0.270	6.579	0.191	6.708	0.188
^{135}I	1260.409	6.580	0.270	6.538	0.270	6.559	0.191	6.708	0.188
^{135}I	1457.560	6.309	0.263	6.328	0.266	6.319	0.187	6.708	0.188
^{135}I	1502.790	6.074	0.301	6.129	0.308	6.101	0.215	6.708	0.188
^{135}I	1566.410	5.870	0.285	5.638	0.278	5.751	0.199	6.708	0.188
^{135}I	1678.027	6.222	0.290	6.108	0.288	6.165	0.204	6.708	0.188
^{135}I	1706.459	6.127	0.307	5.970	0.303	6.047	0.216	6.708	0.188
^{140}Ba	537.261	5.488	0.145	5.488	0.146	5.488	0.103	5.488	0.110
^{141}La	1354.520	5.914	0.311	5.777	0.307	5.845	0.218	5.341	0.427
^{142}La	641.285	5.619	0.156	5.678	0.158	5.648	0.111	4.794	0.134
^{142}La	894.900	5.570	0.207	5.473	0.204	5.521	0.146	4.794	0.134
^{142}La	1043.700	5.552	0.316	5.402	0.391	5.493	0.246	4.794	0.134
^{142}La	1545.800	4.443	0.315	4.070	0.269	4.227	0.205	4.794	0.134
^{142}La	1901.300	4.105	0.166	4.099	0.172	4.102	0.120	4.794	0.134
^{142}La	2397.800	3.899	0.157	3.725	0.158	3.813	0.112	4.794	0.134
^{142}La	2542.700	3.184	0.139	3.383	0.154	3.274	0.103	4.794	0.134
^{143}Ce	293.266	4.420	0.121	4.341	0.119	4.380	0.085	4.650	0.186
^{143}Ce	350.619	5.256	0.156	5.234	0.157	5.245	0.111	4.650	0.186
^{143}Ce	490.368	4.507	0.140	4.526	0.143	4.516	0.100	4.650	0.186
^{143}Ce	721.929	4.993	0.141	4.963	0.141	4.978	0.100	4.650	0.186
^{143}Ce	880.460	4.313	0.187	4.235	0.190	4.275	0.133	4.650	0.186
^{151}Pm	717.720	0.689	0.056	0.411	0.030	0.474	0.026	0.727	0.029

TABLE IX: Np2 cumulative fission product yield results from detectors 8815 and 8816. Values were combined by an uncertainty weighted mean. Reference values are from ENDF/B-VIII.0 [37]. Np1 + Np3's ^{142}La fission product yield result for 894.9 keV γ-ray was used to determine the total number of fission events.

Isotope	E_γ (keV)	FPY_{8815} (%)	ΔFPY_{8815} (%)	FPY_{8816} (%)	ΔFPY_{8816} (%)	$\overline{FPY}$ (%)	$\Delta\overline{FPY}$ (%)	FPY_{ref} (%)	ΔFPY_{ref} (%)
^{88}Kr	196.301	2.320	0.161	2.216	0.152	2.265	0.111	2.096	0.126
^{88}Kr	2195.842	1.832	0.120	1.675	0.111	1.748	0.081	2.096	0.126
^{88}Kr	2392.110	1.772	0.113	1.702	0.111	1.736	0.079	2.096	0.126
^{91}Sr	749.800	4.086	0.214	4.126	0.217	4.106	0.152	3.925	0.157
^{92}Sr	1383.930	4.545	0.340	4.357	0.327	4.447	0.236	3.012	0.084

^{93}Y	266.900	6.597	1.000	6.288	0.954	6.435	0.690	4.371	0.175
^{105}Ru	316.440	3.138	0.174	3.006	0.167	3.070	0.121	3.103	0.186
^{105}Ru	393.360	3.546	0.174	3.464	0.176	3.506	0.124	3.103	0.186
^{105}Ru	469.370	3.615	0.183	3.483	0.178	3.548	0.128	3.103	0.186
^{105}Rh	319.231	2.955	0.186	2.532	0.173	2.728	0.127	3.104	0.087
^{127}Sn	1095.600	0.251	0.074	0.234	0.069	0.242	0.051	0.258	0.082
^{127}Sn	1114.300	0.321	0.069	0.288	0.062	0.303	0.046	0.258	0.082
^{128}Sn	482.300	0.624	0.075	0.606	0.073	0.615	0.052	0.635	0.406
^{130}Sb	330.914	0.889	0.061	0.889	0.061	0.889	0.043	1.169	0.748
^{130}Sb	793.400	0.974	0.065	0.973	0.065	0.973	0.046	1.169	0.748
^{132}Te	228.160	5.745	0.346	4.963	0.296	5.293	0.225	4.751	0.190
^{133m}Te	863.955	3.661	0.347	3.677	0.349	3.669	0.246	3.587	0.287
^{133m}Te	912.671	4.509	0.419	4.430	0.412	4.469	0.294	3.587	0.287
^{133m}Te	1683.230	3.852	0.376	3.524	0.346	3.675	0.255	3.587	0.287
^{134}Te	201.235	4.646	0.316	4.479	0.301	4.559	0.218	4.415	0.177
^{134}Te	712.970	4.869	0.661	8.888	1.212	5.791	0.580	4.415	0.177
^{131}I	364.489	3.534	0.177	3.396	0.181	3.467	0.127	3.600	0.072
^{135}I	220.502	8.088	0.509	8.400	0.533	8.237	0.368	6.708	0.188
^{135}I	288.451	7.635	0.437	6.670	0.382	7.088	0.287	6.708	0.188
^{135}I	1131.511	7.045	0.360	6.926	0.356	6.985	0.253	6.708	0.188
^{135}I	1260.409	6.886	0.352	6.691	0.345	6.787	0.246	6.708	0.188
^{139}Ba	165.857	7.427	0.460	7.038	0.419	7.214	0.310	5.634	0.225
^{142}La	641.285	5.795	0.237	5.622	0.231	5.707	0.166	4.794	0.134
^{142}La	894.900	5.510	0.249	5.510	0.250	5.510	0.176	4.794	0.134
^{142}La	1043.700	6.209	0.308	5.737	0.292	5.961	0.212	4.794	0.134
^{142}La	1233.100	5.302	0.274	5.624	0.293	5.452	0.200	4.794	0.134
^{142}La	1901.300	4.746	0.226	4.449	0.216	4.591	0.156	4.794	0.134
^{142}La	2055.200	4.860	0.307	4.215	0.274	4.500	0.204	4.794	0.134
^{142}La	2100.400	3.745	0.414	3.472	0.384	3.598	0.282	4.794	0.134
^{142}La	2187.200	5.222	0.269	5.049	2.438	5.220	0.267	4.794	0.134
^{142}La	2542.700	3.600	0.184	3.433	0.180	3.515	0.129	4.794	0.134
^{143}Ce	293.266	4.558	0.196	4.341	0.188	4.445	0.136	4.650	0.186

VI. FISSION PRODUCT YIELD ANALYSIS

This section describes how each γ-ray peak was fitted and the time chosen for the decay curve fit. The uncertainty budgets are tabulated in Section VII.

A. ^{88}Kr ($\tau_{1/2} = 2.825 \pm 0.019$ h [1])

Six γ-ray peaks from Np1 + Np3 were analyzed. For the 834.8 keV γ ray, a multi-peak fit routine was used to account for an interfering γ ray at 836.9 keV. The decay curve fit was between 6 and 20 hours. The residual of the fit was within 10%. For the 1518.4 keV γ ray, a multi-peak fit routine was used to account for an interfering γ ray at 1515.6 keV. The decay curve fit was between 6 and 20 hours. The residual of the fit was within 20%. For the 1529.8 keV γ ray, a single-peak fit routine was used. The decay curve fit was between 6 and 20 hours. The residual of the fit was within 15%. For the 2029.8 keV γ ray, a single-peak fit routine was used. The decay curve fit was between 6 and 20 hours. The residual of the fit was within 20%. For the 2195.8 keV γ ray, a single-peak fit routine was used. The decay curve fit was between 6 and 20 hours. The residual of the fit was within 10%. For the 2392.1 keV γ ray, a single-peak fit routine was used. The decay curve fit was between 6 and 20 hours. The residual of the fit was within 10%.

Three γ-ray peaks from Np2 were analyzed. For the 196.3 keV γ ray, a multi-peak fit routine was used to account for an interfering γ ray at 195.1 keV. The decay curve fit was between 1.8 and 3.8 hours. The residual of the fit was within 5%. For the 2195.8 keV γ ray, a single-peak fit routine was used. The decay curve fit was between 2.1 and 3.8 hours. The residual of the fit was within 15%. For the 2392.1 keV γ ray, a single-peak fit routine was used. The decay curve fit was between 1.0 and 3.8 hours. The residual of the fit was within 10%.

B. ^{91}Sr ($\tau_{1/2} = 9.65 \pm 0.06$ h [2])

One γ-ray peaks from Np1 + Np3 was analyzed. For the 749.8 keV γ ray, a single-peak fit routine was used. The decay curve fit was between 6 and 55 hours. The residual of the fit was within 15%.

One γ-ray peaks from Np2 was analyzed. For the 749.8 keV γ ray, a single-peak fit routine was used. The decay curve fit was between 1.3 and 3.8 hours. The residual of the fit was within 7%.

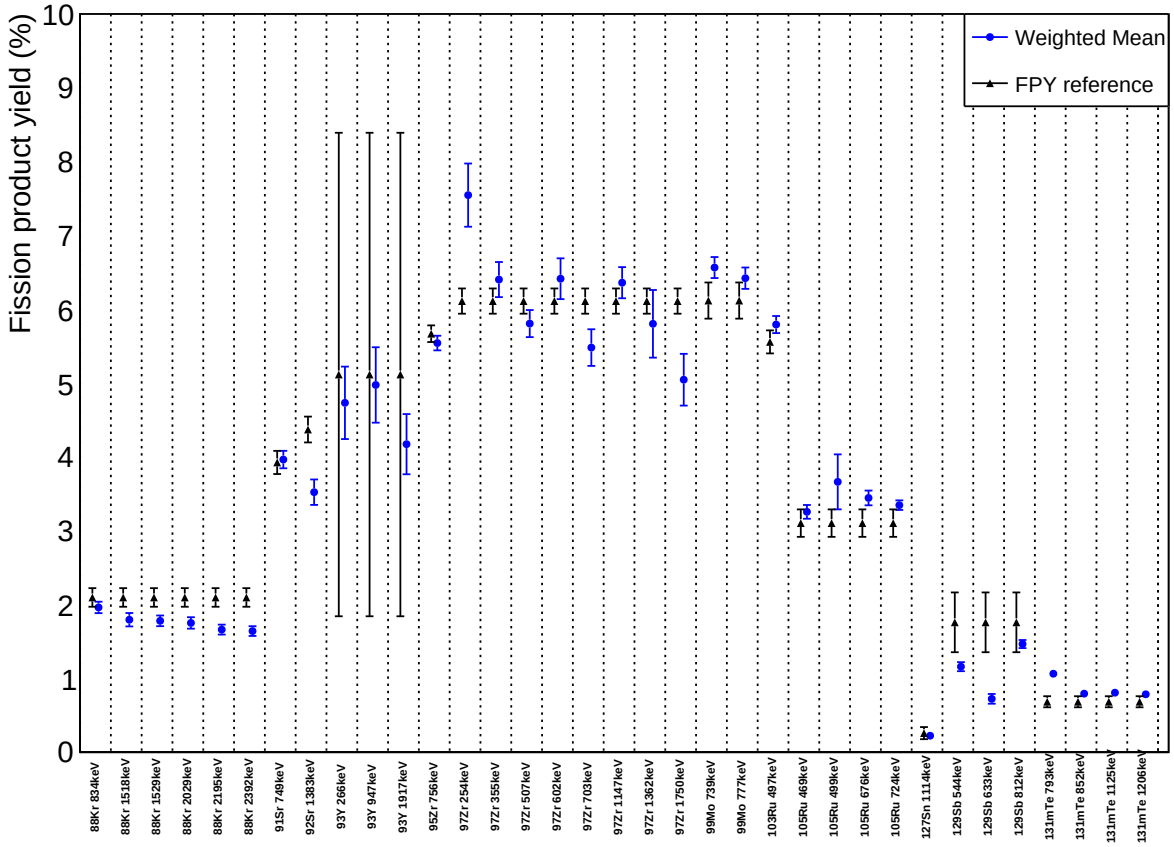

FIG. 15. Np1 + Np3 weighted mean fission product yield results compared to evaluated England and Rider values. (part 1)

C. ^{92}Sr ($\tau_{1/2} = 2.611 \pm 0.017$ h [3])

One γ-ray peak from Np1 + Np3 was analyzed. For the 1383.9 keV γ ray, a single-peak fit routine was used. The decay curve fit was between 17 and 30 hours. The residual of the fit was within 20%.

One γ-ray peak from Np2 was analyzed. For the 1383.9 keV γ ray, a single-peak fit routine was used. The decay curve fit was between 1.0 and 4.0 hours. The residual of the fit was within 5%.

D. ^{93}Y ($\tau_{1/2} = 10.18 \pm 0.08$ h [4])

Three γ-ray peaks from Np1 + Np3 were analyzed. For the 266.9 keV γ ray, a single-peak fit routine was used. The decay curve fit was between 8 and 32 hours. The residual of the fit was within 15%. For the 947.1 keV γ ray, a single-peak fit routine was used. The decay curve fit was between 8 and 30 hours. The residual of the fit was within 15%. For the 1917.8 keV γ ray, a multi-peak fit routine was used to account for an interfering γ-ray at 1921.4 keV. The decay curve fit was between 6 and 30 hours. The residual of the fit was within 15%.

One γ-ray peaks from Np2 was analyzed. For the 266.9 keV γ ray, a single-peak fit routine was used. The decay curve fit was between 2.8 and 3.8 hours. The residual of the fit was within 10%.

E. ^{95}Zr ($\tau_{1/2} = 64.032 \pm 0.006$ d [5])

One γ-ray peak from Np1 + Np3 was analyzed. For the 756.7 keV γ ray, a multi-peak fit routine was used to account for an interfering γ-ray at 753.8 keV. The decay curve fit was between 6 and 120 hours. The residual of the fit was within 20%.

F. ^{97}Zr ($\tau_{1/2} = 16.749 \pm 0.008$ h [6])

Eight γ-ray peaks from Np1 + Np3 were analyzed. For the 254.2 keV γ ray, a single-peak fit routine was used. The decay curve fit was between 9 and 20 hours. The residual of the fit was within 15%. For the 355.4 keV γ ray, a single-peak fit routine was used. The decay curve fit was between 6 and 20 hours. The residual of the fit was within 15%. For the 507.6 keV γ ray, a multi-peak

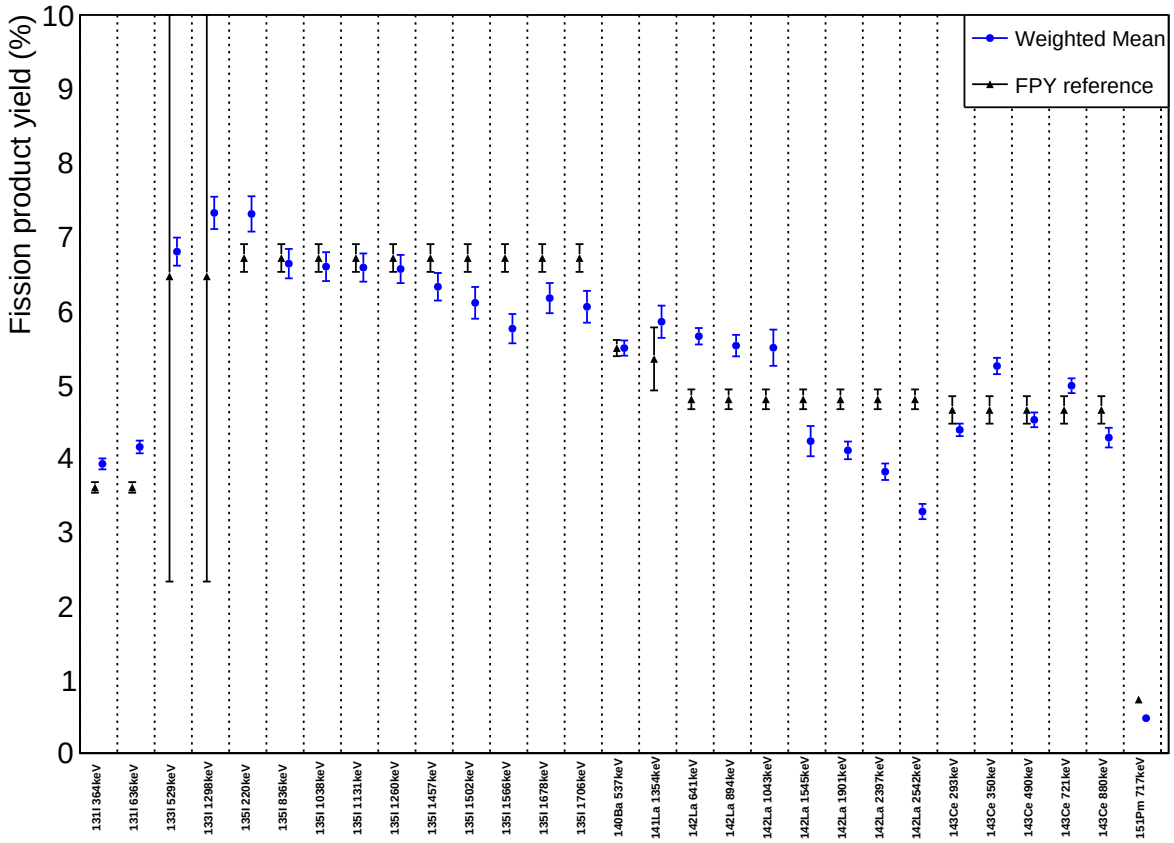

FIG. 16. Np1 + Np3 weighted mean fission product yield results compared to evaluated England and Rider values. (part 2)

fit routine was used to account for an interfering γ ray at 506.1 and 510.6 keV. The decay curve fit was between 6 and 70 hours. The residual of the fit was within 15%. For the 602.4 keV γ ray, a multi-peak fit routine was used to account for an interfering γ ray at 599.9, 605.0, and 607.1 keV. The decay curve fit was between 6 and 31 hours. The residual of the fit was within 15%. For the 703.8 keV γ ray, a multi-peak fit routine was used to account for an interfering γ ray at 706.8 keV. The decay curve fit was between 20 and 30 hours. The residual of the fit was within 15%. For the 1148.0 keV γ ray, a multi-peak fit routine was used to account for an interfering γ ray at 1142.2 and 1143.9 keV. The decay curve fit was between 6 and 48 hours. The residual of the fit was within 15%. For the 1362.7 keV γ ray, a single-peak fit routine was used. The decay curve fit was between 40 and 50 hours. The residual of the fit was within 20%. For the 1750.2 keV γ ray, a single-peak fit routine was used. The decay curve fit was between 6 and 50 hours. The residual of the fit was within 15%.

G. ^{99}Mo ($\tau_{1/2} = 65.924 \pm 0.006$ h [7])

Two γ-ray peaks from Np1 + Np3 were analyzed. For the 739.5 keV γ ray, a single-peak fit routine was used. The decay curve fit was between 20 and 180 hours. The residual of the fit was within 15%. For the 777.9 keV γ ray, a single-peak fit routine was used. The decay curve fit was between 30 and 170 hours. The residual of the fit was within 20%.

H. ^{103}Ru ($\tau_{1/2} = 39.249 \pm 0.003$ d [8])

One γ-ray peak from Np1 + Np3 was analyzed. For the 497.1 keV γ ray, a single-peak fit routine was used. The decay curve fit was between 30 and 180 hours. The residual of the fit was within 10%.

I. ^{105}Ru ($\tau_{1/2} = 4.439 \pm 0.011$ h [9])

Four γ-ray peaks from Np1 + Np3 were analyzed. For the 469.4 keV γ ray, a single-peak fit routine was used. The decay curve fit was between 6 and 20 hours. The

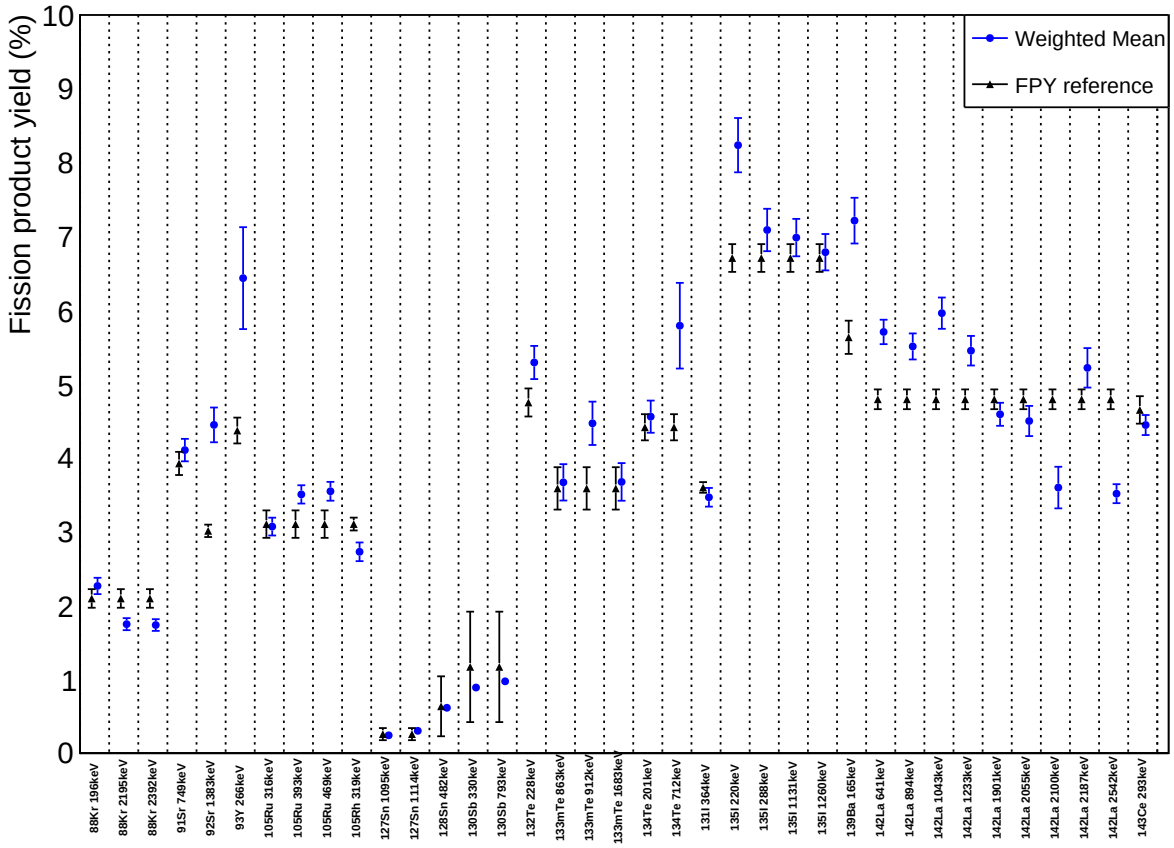

FIG. 17. Np2 weighted mean fission product yield results compared to evaluated England and Rider values.

residual of the fit was within 5%. For the 499.3 keV γ ray, a multi-peak fit routine was used to account for an interfering γ ray at 497.0 keV. The decay curve fit was between 6 and 21 hours. The residual of the fit was within 10%. For the 676.4 keV γ ray, a single-peak fit routine was used. The decay curve fit was between 6 and 20 hours. The residual of the fit was within 5%. For the 724.3 keV γ ray, a multi-peak fit routine was used to account for an interfering γ ray at 721.7 and 727.4 keV. The decay curve fit was between 6 and 19 hours. The residual of the fit was within 3%.

Three γ ray peaks from Np2 were analyzed. For the 316.4 keV γ ray, a single-peak fit routine was used. The decay curve fit was between 2.5 and 3.8 hours. The residual of the fit was within 10%. For the 393.4 keV γ ray, a single-peak fit routine was used. The decay curve fit was between 1.8 and 3.8 hours. The residual of the fit was within 15%. For the 469.4 keV γ ray, a multi-peak fit routine was used to account for an interfering γ ray at 471.8 keV. The decay curve fit was between 1.5 and 3.2 hours. The residual of the fit was within 5%.

J. ^{105}Rh ($\tau_{1/2} = 35.341 \pm 0.019$ h [9])

One γ-ray peak from Np2 was analyzed. For the 319.2 keV γ ray, a single-peak fit routine was used. The decay curve fit was between 2.5 and 3.8 hours. The residual of the fit was within 20%.

K. ^{127}Sn ($\tau_{1/2} = 2.10 \pm 0.04$ h [10])

One γ-ray peak from Np1 + Np3 was analyzed. For the 1114.3 keV γ ray, a single-peak fit routine was used. The decay curve fit was between 6 and 10 hours. The residual of the fit was within 5%.

Two γ-ray peaks from Np2 were analyzed. For the 1095.6 keV γ ray, a single-peak fit routine was used. The decay curve fit was between 1.1 and 1.8 hours. The residual of the fit was within 20%. For the 1114.3 keV γ ray, a single-peak fit routine was used. The decay curve fit was between 0.8 and 3.8 hours. The residual of the fit was within 20%.

L. ^{128}Sn ($\tau_{1/2} = 9.05 \pm 0.04$ **h** [11])

One γ-ray peak from Np2 was analyzed. For the 482.3 keV γ ray, a single-peak fit routine was used. The decay curve fit was between 1.0 and 3.8 hours. The residual of the fit was within 5%.

M. ^{129}Sb ($\tau_{1/2} = 4.366 \pm 0.026$ **h** [12])

Three γ-ray peaks from Np1 + Np3 was analyzed. For the 544.7 keV γ ray, a single-peak fit routine was used. The decay curve fit was between 4 and 8 hours. The residual of the fit was within 2%. For the 633.7 keV γ ray, a single-peak fit routine was used. The decay curve fit was between 4 and 10 hours. The residual of the fit was within 20%. For the 812.8 keV γ-ray, a multi-peak fit routine was used to account for an interfering γ-ray at 809.6 keV. The decay curve fit was between 4 and 10 hours. The residual of the fit was within 1%.

N. ^{130}Sb ($\tau_{1/2} = 39.5 \pm 0.8$ **m** [13])

Two γ-ray peaks from Np2 were analyzed. 1 For the 330.9 keV γ ray, a single-peak fit routine was used. The decay curve fit was between 0.8 and 1.5 hours. The residual of the fit was within 5%. For the 793.4 keV γ ray, a single-peak fit routine was used. The decay curve fit was between 0.8 and 1.2 hours. The residual of the fit was within 5%.

O. ^{131m}Te ($\tau_{1/2} = 33.25 \pm 0.25$ **h** [14])

Four γ-rays from Np1 + Np3 were analyzed. For the 793.8 keV γ ray, a single-peak fit routine was used. The decay curve fit was between 10 and 80 hours. The residual of the fit was within 20%. For the 852.2 keV γ ray, a single-peak fit routine was used. The decay curve fit was between 20 and 60 hours. The residual of the fit was within 20%. For the 1125.5 keV γ ray, a single-peak fit routine was used. The decay curve fit was between 60 and 80 hours. The residual of the fit was within 20%. For the 1206.6 keV γ ray, a single-peak fit routine was used. The decay curve fit was between 20 and 60 hours. The residual of the fit was within 20%.

P. ^{132}Te ($\tau_{1/2} = 3.204 \pm 0.013$ **d** [15])

One γ-ray from Np2 was analyzed. For the 228.2 keV γ ray, a single-peak fit routine was used. The decay curve fit was between 1.0 and 3.8 hours. The residual of the fit was within 20%.

Q. ^{133m}Te ($\tau_{1/2} = 55.4 \pm 0.4$ **m** [16])

Three γ-ray peaks from Np2 were analyzed. For the 864.0 keV γ ray, a multi-peak fit routine was used to account for an interfering γ ray at 861.7 keV. The decay curve fit was between 0.8 and 1.3 hours. The residual of the fit was within 2%. For the 912.7 keV γ ray, a multi-peak fit routine was used to account for an interfering γ ray at 914.7 keV. The decay curve fit was between 0.8 and 1.5 hours. The residual of the fit was within 2%. For the 1683.2 keV γ ray, a single-peak fit routine was used. The decay curve fit was between 1.0 and 3.8 hours. The residual of the fit was within 15%.

R. ^{134}Te ($\tau_{1/2} = 41.8 \pm 0.8$ **m** [17])

Two γ-ray peaks from Np2 were analyzed. For the 201.2 keV γ ray, a single-peak fit routine was used. The decay curve fit was between 0.8 and 2.0 hours. The residual of the fit was within 5%. For the 713.0 keV γ ray, a single-peak fit routine was used. The decay curve fit was between 0.8 and 2.0 hours. The residual of the fit was within 15%.

S. ^{131}I ($\tau_{1/2} = 8.0252 \pm 0.0006$ **d** [14])

Two γ-ray peaks from Np1 + Np3 were analyzed. For the 364.5 keV γ ray, a single-peak fit routine was used. The decay curve fit was between 120 and 180 hours. The residual of the fit was within 5%. For the 364.5 keV γ ray, a single-peak fit routine was used. The decay curve fit was between 60 and 180 hours. The residual of the fit was within 20%.

One γ-ray peak from Np2 was analyzed. For the 364.5 keV γ ray, a multi-peak fit routine was used to account for an interfering γ ray at 362.5 keV. The decay curve fit was between 1.8 and 3.8 hours. The residual of the fit was within 15%.

T. ^{133}I ($\tau_{1/2} = 20.83 \pm 0.08$ **h** [16])

Two γ-ray peaks from Np1 + Np3 were analyzed. For the 529.9 keV γ ray, a multi-peak fit routine was used to account for an interfering γ ray at 526.5 keV. The decay curve fit was between 6 and 130 hours. The residual of the fit was within 3%. For the 1298.2 keV γ ray, a multi-peak fit routine was used to account for an interfering γ ray at 1295.8 keV. The decay curve fit was between 20 and 40 hours. The residual of the fit was within 10%.

U. ^{135}I ($\tau_{1/2} = 6.58 \pm 0.03$ **h** [18])

Ten γ-ray peaks from Np1 + Np3 were analyzed. For the 220.5 keV γ ray, a multi-peak fit routine was used to

account for an interfering γ ray at 222.8 keV. The decay curve fit was between 6 and 20 hours. The residual of the fit was within 15%. For the 836.8 keV γ ray, a multi-peak fit routine was used to account for an interfering γ ray at 834.9 keV. The decay curve fit was between 6 and 30 hours. The residual of the fit was within 5%. For the 1038.8 keV γ ray, a single-peak fit routine was used. The decay curve fit was between 6 and 50 hours. The residual of the fit was within 10%. For the 1131.5 keV γ ray, a single-peak fit routine was used. The decay curve fit was between 6 and 50 hours. The residual of the fit was within 10%. For the 1260.4 keV γ ray, a single-peak fit routine was used. The decay curve fit was between 6 and 60 hours. The residual of the fit was within 10%. For the 1457.6 keV γ ray, a multi-peak fit routine was used to account for an interfering γ ray at 1460.8 keV. The decay curve fit was between 8 and 50 hours. The residual of the fit was within 5%. For the 1502.8 keV γ ray, a single-peak fit routine was used. The decay curve fit was between 6 and 30 hours. The residual of the fit was within 20%. For the 1566.4 keV γ ray, a single-peak fit routine was used. The decay curve fit was between 6 and 40 hours. The residual of the fit was within 20%. For the 1678.0 keV γ ray, a single-peak fit routine was used. The decay curve fit was between 6 and 40 hours. The residual of the fit was within 7%. For the 1706.5 keV γ ray, a single-peak fit routine was used. The decay curve fit was between 6 and 50 hours. The residual of the fit was within 20%.

Four γ-ray peaks from Np2 were analyzed. For the 220.5 keV γ ray, a single-peak fit routine was used. The decay curve fit was between 1.0 and 3.8 hours. The residual of the fit was within 20%. For the 288.5 keV γ ray, a single-peak fit routine was used. The decay curve fit was between 1.5 and 3.8 hours. The residual of the fit was within 20%. For the 1131.5 keV γ ray, a single-peak fit routine was used. The decay curve fit was between 1.0 and 2.8 hours. The residual of the fit was within 5%. For the 1260.4 keV γ ray, a single-peak fit routine was used. The decay curve fit was between 1.0 and 2.8 hours. The residual of the fit was within 5%.

V. ^{139}Ba ($\tau_{1/2} = 82.93 \pm 0.09$ **m** [**19**])

One γ-ray peak from Np2 was analyzed. For the 165.9 keV γ ray, a multi-peak fit routine was used to account for an interfering γ ray at 168.8 keV. The decay curve fit was between 0.8 and 4.0 hours. The residual of the fit was within 5%.

W. ^{140}Ba ($\tau_{1/2} = 12.751 \pm 0.004$ **d** [**20**])

One γ-ray peaks from Np1 + Np3 was analyzed. For the 537.3 keV γ ray, a single-peak fit routine was used. The decay curve fit was between 6 and 180 hours. The residual of the fit was within 15%.

X. ^{141}La ($\tau_{1/2} = 3.92 \pm 0.03$ **h** [**21**])

One γ-ray peak from Np1 + Np3 was analyzed. For the 1354.5 keV γ ray, a single-peak fit routine was used. The decay curve fit was between 6 and 20 hours. The residual of the fit was within 10%.

Y. ^{142}La ($\tau_{1/2} = 91.1 \pm 0.5$ **m** [**22**])

Seven γ-ray peaks from Np1 + Np3 were analyzed. For the 641.3 keV γ ray, a single-peak fit routine was used. The decay curve fit was between 6 and 10 hours. The residual of the fit was within 5%. For the 894.9 keV γ ray, a multi-peak fit routine was used to account for an interfering γ ray at 898.1 keV. The decay curve fit was between 6 and 10 hours. The residual of the fit was within 20%. For the 1043.7 keV γ ray, a single-peak fit routine was used. The decay curve fit was between 6 and 11 hours. The residual of the fit was within 20%. For the 1545.8 keV γ ray, a multi-peak fit routine was used to account for an interfering γ ray at 1543.9 keV. The decay curve fit was between 6 and 12 hours. The residual of the fit was within 20%. For the 1901.3 keV γ ray, a single-peak fit routine was used. The decay curve fit was between 6 and 10 hours. The residual of the fit was within 7%. For the 2397.8 keV γ ray, a multi-peak fit routine was used to account for an interfering γ ray at 2392.6 keV. The decay curve fit was between 6 and 10 hours. The residual of the fit was within 10%. For the 1901.3 keV γ ray, a single-peak fit routine was used. The decay curve fit was between 6 and 16 hours. The residual of the fit was within 20%.

Nine γ-ray peaks from Pu1 were analyzed. For the 641.3 keV γ ray, a single-peak fit routine was used. The decay curve fit was between 2.0 and 3.8 hours. The residual of the fit was within 3%. For the 849.9 keV γ ray, a multi-peak fit routine was used to account for an interfering γ ray at 898.0 keV. The decay curve fit was between 1.8 and 3.2 hours. The residual of the fit was within 3%. For the 1043.7 keV γ ray, a multi-peak fit routine was used to account for an interfering γ ray at 1052.5 keV. The decay curve fit was between 1.5 and 2.3 hours. The residual of the fit was within 10%. For the 1233.1 keV γ ray, a single-peak fit routine was used. The decay curve fit was between 0.8 and 3.8 hours. The residual of the fit was within 20%. For the 1901.3 keV γ ray, a multi-peak fit routine was used to account for an interfering γ ray at 1898.0 keV. The decay curve fit was between 0.8 and 3.8 hours. The residual of the fit was within 10%. For the 2055.2 keV γ ray, a single-peak fit routine was used. The decay curve fit was between 1.0 and 3.8 hours. The residual of the fit was within 20%. For the 2100.4 keV γ ray, a single-peak fit routine was used. The decay curve fit was between 1.8 and 3.5 hours. The residual of the fit was within 15%. For the 2187.2 keV γ ray, a single-peak fit routine was used. The decay curve fit was between 1.0 and 4.0 hours. The residual of the fit was within 15%.

For the 2542.7 keV γ ray, a single-peak fit routine was used. The decay curve fit was between 0.8 and 4.0 hours. The residual of the fit was within 10%.

Z. ^{143}Ce ($\tau_{1/2} = 33.039 \pm 0.006$ h [23])

Five γ-ray peaks from Np1 + Np3 were analyzed. For the 293.3 keV γ ray, a single-peak fit routine was used. The decay curve fit was between 6 and 120 hours. The residual of the fit was within 5%. For the 350.6 keV γ ray, a multi-peak fit routine was used to account for an interfering γ ray at 351.7 keV. The decay curve fit was between 10 and 40 hours. The residual of the fit was within 15%. For the 490.4 keV γ-ray, a multi-peak fit routine was used to account for an interfering γ-ray at 492.7 keV. The decay curve fit was between 13 and 60 hours. The residual of the fit was within 15%. For the 721.9 keV γ-ray, a multi-peak fit routine was used to ccount for an interfering γ-ray at 724.2 and 727.3 keV. The decay curve fit was between 6 and 47 hours. The residual of the fit was within 15%. For the 880.5 keV γ-ray, a multi-peak fit routine was used to account for an interfering γ-ray at 882.8 keV. The decay curve fit was between 35 and 60 hours. The residual of the fit was within 15%.

One γ-ray peak from Np2 was analyzed. For the 293.3 keV γ ray, a single-peak fit routine was used. The decay curve fit was between 1.3 and 3.8 hours. The residual of the fit was within 10%.

AA. ^{151}Pm ($\tau_{1/2} = 28.40 \pm 0.04$ h [24])

One γ-ray peak from Np1 + Np3 was analyzed. For the 717.7 keV γ ray, a multi-peak fit routine was used to account for an interfering γ ray at 713.1 and 715.6 keV. The decay curve fit was between 6 and 50 hours. The residual of the fit was within 20%.

VII. FISSION PRODUCT YIELD PARAMETER AND UNCERTAINTY BUDGET

TABLE X: Values used to calculate Np1 + Np3 cumulative fission product yield results and uncertainties for detector 8815 where N_f = 1.81E10 ± 4E8.

Isotope	E_γ (keV)	A_0 (Bq)	ΔA_0 (Bq)	$\tau_{1/2}$ (hrs.)	$\Delta\tau_{1/2}$ (hrs.)	ϵ_γ	$\Delta\epsilon_\gamma$	I_γ	ΔI_γ	R_γ (%)	ΔR_γ (%)
^{88}Kr	834.830	1.263E+01	1.311E-01	2.840	0.030	4.060E-03	1.746E-05	9.935E-01	1.203E-03	12.975	0.616
^{88}Kr	1518.390	1.264E+00	4.949E-02	2.840	0.030	2.796E-03	2.692E-05	9.962E-01	7.049E-04	2.152	0.114
^{88}Kr	1529.770	6.697E+00	6.707E-02	2.840	0.030	2.785E-03	2.709E-05	9.962E-01	7.019E-04	10.934	0.534
^{88}Kr	2029.840	2.358E+00	4.818E-02	2.840	0.030	2.422E-03	3.412E-05	9.966E-01	6.229E-04	4.529	0.227
^{88}Kr	2195.842	6.243E+00	5.616E-02	2.840	0.030	2.340E-03	3.639E-05	9.967E-01	6.089E-04	13.183	0.618
^{88}Kr	2392.110	1.568E+01	8.015E-02	2.840	0.030	2.257E-03	3.901E-05	9.968E-01	5.962E-04	34.600	1.603
^{91}Sr	749.800	1.478E+01	3.047E-02	9.630	0.050	4.387E-03	1.641E-05	9.926E-01	1.360E-03	23.685	0.796
^{92}Sr	1383.930	1.202E+02	1.245E+00	2.710	0.010	2.942E-03	2.501E-05	9.960E-01	7.467E-04	90.000	5.682
^{93}Y	266.900	1.170E+01	7.161E-02	10.180	0.080	1.036E-02	1.242E-05	9.561E-01	7.965E-03	7.320	1.054
^{93}Y	947.100	1.291E+00	1.590E-02	10.180	0.080	3.721E-03	1.892E-05	9.943E-01	1.047E-03	2.093	0.298
^{93}Y	1917.800	5.390E-01	5.369E-03	10.180	0.080	2.486E-03	3.257E-05	9.966E-01	6.344E-04	1.545	0.208
^{95}Zr	756.725	2.923E-01	2.347E-04	1536.768	0.144	4.357E-03	1.649E-05	9.927E-01	1.346E-03	54.380	0.220
^{97}Zr	254.170	1.753E+00	6.024E-02	16.749	0.008	1.079E-02	1.239E-05	9.510E-01	8.860E-03	1.145	0.075
^{97}Zr	355.400	2.238E+00	2.667E-02	16.749	0.008	8.081E-03	1.279E-05	9.758E-01	4.435E-03	2.095	0.093
^{97}Zr	507.640	3.579E+00	1.318E-02	16.749	0.008	5.953E-03	1.386E-05	9.872E-01	2.362E-03	5.027	0.186
^{97}Zr	602.370	1.005E+00	8.214E-03	16.749	0.008	5.184E-03	1.476E-05	9.901E-01	1.820E-03	1.378	0.075
^{97}Zr	703.760	5.280E-01	1.850E-02	16.749	0.008	4.599E-03	1.587E-05	9.920E-01	1.470E-03	1.015	0.047
^{97}Zr	1147.970	1.138E+00	6.094E-03	16.749	0.008	3.286E-03	2.167E-05	9.953E-01	8.634E-04	2.616	0.102
^{97}Zr	1362.680	3.661E-01	1.425E-02	16.749	0.008	2.968E-03	2.470E-05	9.959E-01	7.546E-04	1.024	0.102
^{97}Zr	1750.240	3.004E-01	2.998E-03	16.749	0.008	2.598E-03	3.022E-05	9.965E-01	6.567E-04	1.089	0.102
^{99}Mo	739.500	1.882E+00	4.057E-03	65.976	0.024	4.432E-03	1.628E-05	9.925E-01	1.383E-03	12.260	0.218
^{99}Mo	777.921	6.137E-01	3.873E-03	65.976	0.024	4.271E-03	1.675E-05	9.930E-01	1.303E-03	4.303	0.080
^{103}Ru	497.085	1.177E+00	2.089E-03	941.928	0.072	6.058E-03	1.377E-05	9.867E-01	2.443E-03	91.000	1.221
^{105}Ru	469.370	2.788E+01	9.404E-02	4.440	0.020	6.356E-03	1.355E-05	9.854E-01	2.683E-03	17.548	0.552
^{105}Ru	499.300	3.592E+00	6.760E-02	4.440	0.020	6.036E-03	1.379E-05	9.868E-01	2.426E-03	2.034	0.285
^{105}Ru	676.360	2.005E+01	8.273E-02	4.440	0.020	4.739E-03	1.556E-05	9.916E-01	1.548E-03	15.656	0.501
^{105}Ru	724.300	5.567E+01	1.048E-01	4.440	0.020	4.501E-03	1.611E-05	9.923E-01	1.418E-03	47.300	0.500
^{127}Sn	1114.300	4.636E+00	1.758E-01	2.100	0.040	3.348E-03	2.120E-05	9.952E-01	8.872E-04	38.000	7.965
^{129}Sb	544.700	9.250E+00	1.397E-01	4.400	0.010	5.619E-03	1.420E-05	9.885E-01	2.115E-03	18.056	1.234
^{129}Sb	633.700	7.892E-01	6.555E-02	4.400	0.010	4.982E-03	1.509E-05	9.908E-01	1.693E-03	2.771	0.252
^{129}Sb	812.800	2.075E+01	9.428E-02	4.400	0.010	4.138E-03	1.718E-05	9.933E-01	1.240E-03	43.300	2.000
^{131m}Te	793.750	6.075E-01	4.873E-03	33.250	0.250	4.209E-03	1.694E-05	9.931E-01	1.274E-03	13.370	0.297
^{131m}Te	852.210	6.738E-01	5.489E-03	33.250	0.250	4.001E-03	1.768E-05	9.936E-01	1.176E-03	20.279	0.567

^{131m}Te	1125.460	3.122E-01	7.909E-03	33.250	0.250	3.327E-03	2.135E-05	9.953E-01	8.790E-04	11.017	0.294
^{131m}Te	1206.600	2.473E-01	2.898E-03	33.250	0.250	3.188E-03	2.249E-05	9.955E-01	8.273E-04	9.411	0.221
^{131}I	364.489	4.467E+00	8.331E-03	192.605	0.014	7.904E-03	1.284E-05	9.770E-01	4.223E-03	81.500	0.759
^{131}I	636.989	2.618E-01	1.774E-03	192.605	0.014	4.962E-03	1.513E-05	9.909E-01	1.681E-03	7.156	0.100
^{133}I	529.872	5.604E+01	2.792E-02	20.800	0.100	5.747E-03	1.406E-05	9.880E-01	2.208E-03	87.000	2.651
^{133}I	1298.223	8.799E-01	7.186E-03	20.800	0.100	3.052E-03	2.379E-05	9.958E-01	7.812E-04	2.349	0.075
^{135}I	220.502	7.767E+00	8.428E-03	6.570	0.020	1.204E-02	1.232E-05	9.322E-01	1.215E-02	1.751	0.062
^{135}I	836.804	9.499E+00	3.678E-02	6.570	0.020	4.053E-03	1.748E-05	9.935E-01	1.200E-03	6.687	0.227
^{135}I	1038.760	9.692E+00	2.914E-02	6.570	0.020	3.501E-03	2.015E-05	9.949E-01	9.502E-04	7.950	0.264
^{135}I	1131.511	2.600E+01	4.533E-02	6.570	0.020	3.316E-03	2.144E-05	9.953E-01	8.747E-04	22.587	0.723
^{135}I	1260.409	3.089E+01	4.524E-02	6.570	0.020	3.106E-03	2.325E-05	9.957E-01	7.990E-04	28.700	0.916
^{135}I	1457.560	8.237E+00	2.460E-02	6.570	0.020	2.859E-03	2.606E-05	9.961E-01	7.222E-04	8.667	0.278
^{135}I	1502.790	9.683E-01	1.222E-02	6.570	0.020	2.812E-03	2.670E-05	9.962E-01	7.092E-04	1.076	0.043
^{135}I	1566.410	1.099E+00	1.304E-02	6.570	0.020	2.750E-03	2.761E-05	9.963E-01	6.928E-04	1.292	0.050
^{135}I	1678.027	8.317E+00	2.424E-02	6.570	0.020	2.654E-03	2.919E-05	9.964E-01	6.691E-04	9.557	0.361
^{135}I	1706.459	3.487E+00	1.653E-02	6.570	0.020	2.631E-03	2.960E-05	9.964E-01	6.640E-04	4.104	0.172
^{140}Ba	537.261	8.535E-01	2.377E-03	306.065	0.055	5.682E-03	1.413E-05	9.883E-01	2.161E-03	24.390	0.220
^{141}La	1354.520	2.550E+00	3.689E-02	3.920	0.030	2.979E-03	2.459E-05	9.959E-01	7.577E-04	1.640	0.070
^{142}La	641.285	2.983E+02	1.295E+00	1.518	0.008	4.937E-03	1.517E-05	9.910E-01	1.665E-03	47.400	0.500
^{142}La	894.900	4.090E+01	7.471E-01	1.518	0.008	3.868E-03	1.823E-05	9.940E-01	1.114E-03	8.342	0.167
^{142}La	1043.700	1.193E+01	5.542E-01	1.518	0.008	3.490E-03	2.022E-05	9.949E-01	9.456E-04	2.702	0.055
^{142}La	1545.800	8.380E+00	3.674E-01	1.518	0.008	2.769E-03	2.731E-05	9.962E-01	6.979E-04	2.986	0.146
^{142}La	1901.300	1.673E+01	3.047E-01	1.518	0.008	2.497E-03	3.234E-05	9.966E-01	6.362E-04	7.157	0.161
^{142}La	2397.800	2.663E+01	2.997E-01	1.518	0.008	2.255E-03	3.909E-05	9.968E-01	5.958E-04	13.272	0.317
^{142}La	2542.700	1.601E+01	2.623E-01	1.518	0.008	2.203E-03	4.098E-05	9.968E-01	5.888E-04	10.001	0.259
^{143}Ce	293.266	1.834E+01	2.435E-02	33.039	0.006	9.562E-03	1.251E-05	9.641E-01	6.545E-03	42.800	0.420
^{143}Ce	350.619	1.425E+00	1.395E-02	33.039	0.006	8.178E-03	1.276E-05	9.751E-01	4.555E-03	3.231	0.040
^{143}Ce	490.368	6.191E-01	7.989E-03	33.039	0.006	6.127E-03	1.372E-05	9.865E-01	2.497E-03	2.161	0.029
^{143}Ce	721.929	1.268E+00	7.065E-03	33.039	0.006	4.512E-03	1.608E-05	9.923E-01	1.424E-03	5.393	0.066
^{143}Ce	880.460	1.818E-01	6.035E-03	33.039	0.006	3.911E-03	1.804E-05	9.939E-01	1.134E-03	1.031	0.013
^{151}Pm	717.720	1.536E-01	5.473E-03	28.400	0.040	4.531E-03	1.603E-05	9.922E-01	1.434E-03	4.050	0.277

TABLE XI: Values used to calculate Np1 + Np3 cumulative fission product yield results and uncertainties for detector 8816 where N_f = 1.81E10 ± 4E8.

Isotope	E_γ (keV)	A_0 (Bq)	ΔA_0 (Bq)	$\tau_{1/2}$ (hrs.)	$\Delta\tau_{1/2}$ (hrs.)	ϵ_γ	$\Delta\epsilon_\gamma$	I_γ	ΔI_γ	R_γ (%)	ΔR_γ (%)
^{88}Kr	834.830	1.057E+01	1.244E-01	2.840	0.030	3.428E-03	1.620E-05	9.920E-01	1.223E-03	12.975	0.616
^{88}Kr	1518.390	1.173E+00	4.500E-02	2.840	0.030	2.373E-03	2.671E-05	9.953E-01	7.169E-04	2.152	0.114
^{88}Kr	1529.770	5.547E+00	6.071E-02	2.840	0.030	2.364E-03	2.689E-05	9.953E-01	7.139E-04	10.934	0.534
^{88}Kr	2029.840	1.988E+00	4.337E-02	2.840	0.030	2.062E-03	3.430E-05	9.958E-01	6.336E-04	4.529	0.227
^{88}Kr	2195.842	5.344E+00	5.146E-02	2.840	0.030	1.994E-03	3.665E-05	9.959E-01	6.193E-04	13.183	0.618
^{88}Kr	2392.110	1.333E+01	7.364E-02	2.840	0.030	1.926E-03	3.936E-05	9.960E-01	6.064E-04	34.600	1.603
^{91}Sr	749.800	1.246E+01	2.793E-02	9.630	0.050	3.702E-03	1.495E-05	9.909E-01	1.382E-03	23.685	0.796
^{92}Sr	1383.930	1.004E+02	9.906E-01	2.710	0.010	2.495E-03	2.465E-05	9.950E-01	7.593E-04	90.000	5.682
^{93}Y	266.900	9.815E+00	6.893E-02	10.180	0.080	8.729E-03	9.694E-06	9.460E-01	8.022E-03	7.320	1.054
^{93}Y	947.100	1.136E+00	1.095E-02	10.180	0.080	3.145E-03	1.789E-05	9.930E-01	1.065E-03	2.093	0.298
^{93}Y	1917.800	4.712E-01	4.785E-03	10.180	0.080	2.116E-03	3.268E-05	9.958E-01	6.452E-04	1.545	0.208
^{95}Zr	756.725	2.517E-01	4.872E-04	1536.768	0.144	3.677E-03	1.505E-05	9.910E-01	1.368E-03	54.380	0.220
^{97}Zr	254.170	1.636E+00	6.779E-02	16.749	0.008	9.088E-03	9.640E-06	9.398E-01	8.912E-03	1.145	0.075
^{97}Zr	355.400	1.811E+00	2.410E-02	16.749	0.008	6.809E-03	1.025E-05	9.701E-01	4.489E-03	2.095	0.093
^{97}Zr	507.640	2.986E+00	1.236E-02	16.749	0.008	5.017E-03	1.175E-05	9.842E-01	2.397E-03	5.027	0.186
^{97}Zr	602.370	7.514E-01	1.016E-02	16.749	0.008	4.371E-03	1.292E-05	9.878E-01	1.849E-03	1.378	0.075
^{97}Zr	703.760	4.440E-01	1.689E-02	16.749	0.008	3.879E-03	1.430E-05	9.902E-01	1.494E-03	1.015	0.047
^{97}Zr	1147.970	9.511E-01	4.511E-03	16.749	0.008	2.782E-03	2.099E-05	9.942E-01	8.779E-04	2.616	0.102
^{97}Zr	1362.680	3.085E-01	1.457E-02	16.749	0.008	2.517E-03	2.432E-05	9.950E-01	7.673E-04	1.024	0.102
^{97}Zr	1750.240	2.476E-01	2.837E-03	16.749	0.008	2.209E-03	3.021E-05	9.956E-01	6.679E-04	1.089	0.102
^{99}Mo	739.500	1.563E+00	3.738E-03	65.976	0.024	3.740E-03	1.480E-05	9.908E-01	1.405E-03	12.260	0.218
^{99}Mo	777.921	5.252E-01	3.959E-03	65.976	0.024	3.604E-03	1.536E-05	9.913E-01	1.325E-03	4.303	0.080
^{103}Ru	497.085	9.687E-01	2.084E-03	941.928	0.072	5.105E-03	1.163E-05	9.836E-01	2.479E-03	91.000	1.221

^{105}Ru	469.370	2.372E+01	8.729E-02	4.440	0.020	5.355E-03	1.133E-05	9.820E-01	2.721E-03	17.548	0.552
^{105}Ru	499.300	2.840E+00	6.124E-02	4.440	0.020	5.086E-03	1.166E-05	9.837E-01	2.462E-03	2.034	0.285
^{105}Ru	676.360	1.659E+01	8.070E-02	4.440	0.020	3.997E-03	1.391E-05	9.896E-01	1.573E-03	15.656	0.501
^{105}Ru	724.300	4.651E+01	9.646E-02	4.440	0.020	3.797E-03	1.459E-05	9.905E-01	1.441E-03	47.300	0.500
^{127}Sn	1114.300	3.990E+00	1.573E-01	2.100	0.040	2.833E-03	2.047E-05	9.941E-01	9.020E-04	38.000	7.965
^{129}Sb	544.700	7.681E+00	1.453E-01	4.400	0.010	4.736E-03	1.219E-05	9.858E-01	2.147E-03	18.056	1.234
^{129}Sb	633.700	6.516E-01	6.097E-02	4.400	0.010	4.201E-03	1.333E-05	9.887E-01	1.719E-03	2.771	0.252
^{129}Sb	812.800	1.729E+01	9.418E-02	4.400	0.010	3.493E-03	1.587E-05	9.917E-01	1.260E-03	43.300	2.000
^{131m}Te	793.750	5.375E-01	4.723E-03	33.250	0.250	3.553E-03	1.559E-05	9.915E-01	1.295E-03	13.370	0.297
^{131m}Te	852.210	5.605E-01	5.071E-03	33.250	0.250	3.379E-03	1.646E-05	9.921E-01	1.195E-03	20.279	0.567
^{131m}Te	1125.460	2.565E-01	7.054E-03	33.250	0.250	2.816E-03	2.065E-05	9.941E-01	8.938E-04	11.017	0.294
^{131m}Te	1206.600	2.056E-01	2.781E-03	33.250	0.250	2.699E-03	2.190E-05	9.945E-01	8.413E-04	9.411	0.221
^{131}I	364.489	3.730E+00	7.684E-03	192.605	0.014	6.660E-03	1.033E-05	9.716E-01	4.275E-03	81.500	0.759
^{131}I	636.989	2.239E-01	1.606E-03	192.605	0.014	4.185E-03	1.338E-05	9.888E-01	1.707E-03	7.156	0.100
^{133}I	529.872	4.735E+01	2.095E-02	20.800	0.100	4.844E-03	1.201E-05	9.852E-01	2.241E-03	87.000	2.651
^{133}I	1298.223	7.364E-01	6.736E-03	20.800	0.100	2.586E-03	2.333E-05	9.948E-01	7.944E-04	2.349	0.075
^{135}I	220.502	6.167E+00	9.218E-02	6.570	0.020	1.014E-02	9.521E-06	9.168E-01	1.216E-02	1.751	0.062
^{135}I	836.804	7.951E+00	3.422E-02	6.570	0.020	3.422E-03	1.623E-05	9.920E-01	1.220E-03	6.687	0.227
^{135}I	1038.760	8.156E+00	2.681E-02	6.570	0.020	2.961E-03	1.930E-05	9.937E-01	9.660E-04	7.950	0.264
^{135}I	1131.511	2.197E+01	4.428E-02	6.570	0.020	2.806E-03	2.074E-05	9.942E-01	8.894E-04	22.587	0.723
^{135}I	1260.409	2.608E+01	4.164E-02	6.570	0.020	2.631E-03	2.274E-05	9.947E-01	8.125E-04	28.700	0.916
^{135}I	1457.560	7.031E+00	2.289E-02	6.570	0.020	2.425E-03	2.578E-05	9.952E-01	7.345E-04	8.667	0.278
^{135}I	1502.790	8.317E-01	1.129E-02	6.570	0.020	2.386E-03	2.648E-05	9.953E-01	7.212E-04	1.076	0.043
^{135}I	1566.410	8.992E-01	1.183E-02	6.570	0.020	2.335E-03	2.744E-05	9.954E-01	7.046E-04	1.292	0.050
^{135}I	1678.027	6.960E+00	2.208E-02	6.570	0.020	2.255E-03	2.913E-05	9.955E-01	6.805E-04	9.557	0.361
^{135}I	1706.459	2.897E+00	1.509E-02	6.570	0.020	2.236E-03	2.956E-05	9.956E-01	6.753E-04	4.104	0.172
^{140}Ba	537.261	7.203E-01	2.216E-03	306.065	0.055	4.789E-03	1.210E-05	9.855E-01	2.193E-03	24.390	0.220
^{141}La	1354.520	2.119E+00	3.349E-02	3.920	0.030	2.525E-03	2.420E-05	9.949E-01	7.705E-04	1.640	0.070
^{142}La	641.285	2.547E+02	1.205E+00	1.518	0.008	4.163E-03	1.344E-05	9.889E-01	1.691E-03	47.400	0.500
^{142}La	894.900	3.404E+01	6.226E-01	1.518	0.008	3.267E-03	1.710E-05	9.926E-01	1.132E-03	8.342	0.167
^{142}La	1043.700	9.841E+00	6.332E-01	1.518	0.008	2.952E-03	1.938E-05	9.937E-01	9.614E-04	2.702	0.055
^{142}La	1545.800	6.538E+00	2.279E-01	1.518	0.008	2.351E-03	2.713E-05	9.953E-01	7.097E-04	2.986	0.146
^{142}La	1901.300	1.426E+01	2.837E-01	1.518	0.008	2.124E-03	3.244E-05	9.958E-01	6.471E-04	7.157	0.161
^{142}La	2397.800	2.178E+01	2.963E-01	1.518	0.008	1.924E-03	3.943E-05	9.960E-01	6.061E-04	13.272	0.317
^{142}La	2542.700	1.457E+01	2.439E-01	1.518	0.008	1.881E-03	4.138E-05	9.961E-01	5.989E-04	10.001	0.259
^{143}Ce	293.266	1.511E+01	2.287E-02	33.039	0.006	8.056E-03	9.833E-06	9.557E-01	6.605E-03	42.800	0.420
^{143}Ce	350.619	1.193E+00	1.321E-02	33.039	0.006	6.890E-03	1.022E-05	9.693E-01	4.609E-03	3.231	0.040
^{143}Ce	490.368	5.244E-01	7.564E-03	33.039	0.006	5.163E-03	1.156E-05	9.833E-01	2.534E-03	2.161	0.029
^{143}Ce	721.929	1.066E+00	6.782E-03	33.039	0.006	3.807E-03	1.455E-05	9.905E-01	1.447E-03	5.393	0.066
^{143}Ce	880.460	1.512E-01	5.270E-03	33.039	0.006	3.304E-03	1.688E-05	9.924E-01	1.153E-03	1.031	0.013
^{151}Pm	717.720	7.747E-02	5.300E-04	28.400	0.040	3.823E-03	1.449E-05	9.904E-01	1.457E-03	4.050	0.277

TABLE XII: Values used to calculate Np2 cumulative fission product yield results and uncertainties for detector 8815 where N_f = 7.2E9 ± 3E8.

Isotope	E_γ (keV)	A_0 (Bq)	ΔA_0 (Bq)	$\tau_{1/2}$ (hrs.)	$\Delta\tau_{1/2}$ (hrs.)	ϵ_γ	$\Delta\epsilon_\gamma$	I_γ	ΔI_γ	R_γ (%)	ΔR_γ (%)
^{88}Kr	196.301	3.606E+01	1.952E-01	2.840	0.030	1.301E-02	1.230E-05	9.402E-01	2.957E-02	25.985	1.214
^{88}Kr	2195.842	2.757E+00	3.841E-02	2.840	0.030	2.340E-03	3.639E-05	9.978E-01	1.128E-03	13.183	0.618
^{88}Kr	2392.110	6.751E+00	3.809E-02	2.840	0.030	2.257E-03	3.901E-05	9.978E-01	1.104E-03	34.600	1.603
^{91}Sr	749.800	6.092E+00	4.353E-02	9.630	0.050	4.387E-03	1.641E-05	9.950E-01	2.523E-03	23.685	0.796
^{92}Sr	1383.930	6.150E+01	1.087E-01	2.710	0.010	2.942E-03	2.501E-05	9.973E-01	1.383E-03	90.000	5.682
^{93}Y	266.900	6.622E+00	1.397E-01	10.180	0.080	1.036E-02	1.242E-05	9.702E-01	1.496E-02	7.320	1.054
^{105}Ru	316.440	9.559E+00	1.174E-01	4.440	0.020	8.949E-03	1.260E-05	9.792E-01	1.048E-02	11.116	0.396
^{105}Ru	393.360	3.054E+00	7.190E-02	4.440	0.020	7.395E-03	1.301E-05	9.865E-01	6.819E-03	3.775	0.062
^{105}Ru	469.370	1.249E+01	6.129E-03	4.440	0.020	6.356E-03	1.355E-05	9.902E-01	4.988E-03	17.548	0.552
^{105}Rh	319.231	1.928E+00	6.810E-02	35.360	0.060	8.880E-03	1.261E-05	9.796E-01	1.029E-02	19.100	0.630
^{127}Sn	1095.600	1.084E+00	1.264E-01	2.100	0.040	3.384E-03	2.094E-05	9.967E-01	1.671E-03	19.380	5.214
^{127}Sn	1114.300	2.693E+00	4.246E-02	2.100	0.040	3.348E-03	2.120E-05	9.968E-01	1.644E-03	38.000	7.965
^{128}Sn	482.300	3.196E+01	2.079E-01	0.984	0.002	6.212E-03	1.365E-05	9.906E-01	4.769E-03	59.000	6.686

^{130}Sb	330.914	1.236E+02	6.617E-01	0.658	0.013	8.605E-03	1.266E-05	9.811E-01	9.554E-03	78.000	4.000
^{130}Sb	793.400	8.612E+01	6.387E-01	0.658	0.013	4.210E-03	1.694E-05	9.954E-01	2.364E-03	100.000	5.000
^{132}Te	228.160	1.026E+01	7.194E-02	76.896	0.312	1.174E-02	1.234E-05	9.573E-01	2.129E-02	88.000	3.478
^{133m}Te	863.955	3.236E+01	2.970E-01	0.923	0.007	3.963E-03	1.783E-05	9.958E-01	2.147E-03	14.887	1.274
^{133m}Te	912.671	1.128E+02	3.949E-01	0.923	0.007	3.816E-03	1.846E-05	9.960E-01	2.021E-03	43.767	3.666
^{133m}Te	1683.230	6.043E+00	9.466E-02	0.923	0.007	2.650E-03	2.927E-05	9.976E-01	1.238E-03	3.945	0.344
^{134}Te	201.235	9.900E+01	5.924E-01	0.697	0.013	1.281E-02	1.230E-05	9.433E-01	2.807E-02	8.850	0.380
^{134}Te	712.970	2.074E+01	2.773E-01	0.697	0.013	4.554E-03	1.597E-05	9.947E-01	2.683E-03	4.720	0.604
^{131}I	364.489	1.616E+00	4.710E-02	192.605	0.014	7.904E-03	1.284E-05	9.844E-01	7.874E-03	81.500	0.759
^{135}I	220.502	3.437E+00	8.403E-02	6.570	0.020	1.204E-02	1.232E-05	9.538E-01	2.300E-02	1.751	0.062
^{135}I	288.451	4.730E+00	7.465E-02	6.570	0.020	9.699E-03	1.249E-05	9.748E-01	1.268E-02	3.100	0.113
^{135}I	1131.511	1.112E+01	5.921E-02	6.570	0.020	3.316E-03	2.144E-05	9.968E-01	1.621E-03	22.587	0.723
^{135}I	1260.409	1.294E+01	5.724E-02	6.570	0.020	3.106E-03	2.325E-05	9.971E-01	1.481E-03	28.700	0.916
^{139}Ba	165.857	2.286E+02	3.432E-01	1.384	0.005	1.415E-02	1.229E-05	9.120E-01	4.280E-02	23.760	0.250
^{142}La	641.285	1.233E+02	2.921E-01	1.518	0.008	4.937E-03	1.517E-05	9.939E-01	3.090E-03	47.400	0.500
^{142}La	894.900	1.620E+01	1.358E-01	1.518	0.008	3.868E-03	1.823E-05	9.959E-01	2.065E-03	8.342	0.167
^{142}La	1043.700	5.338E+00	1.150E-01	1.518	0.008	3.490E-03	2.022E-05	9.966E-01	1.753E-03	2.702	0.055
^{142}La	1233.100	2.885E+00	5.457E-02	1.518	0.008	3.146E-03	2.286E-05	9.970E-01	1.506E-03	1.896	0.051
^{142}La	1901.300	7.739E+00	5.439E-02	1.518	0.008	2.497E-03	3.234E-05	9.977E-01	1.179E-03	7.157	0.161
^{142}La	2055.200	2.329E+00	3.588E-02	1.518	0.008	2.409E-03	3.447E-05	9.977E-01	1.150E-03	2.180	0.098
^{142}La	2100.400	8.505E-01	3.969E-02	1.518	0.008	2.386E-03	3.509E-05	9.978E-01	1.142E-03	1.043	0.095
^{142}La	2187.200	4.130E+00	4.100E-02	1.518	0.008	2.344E-03	3.627E-05	9.978E-01	1.129E-03	3.697	0.103
^{142}La	2542.700	7.242E+00	4.622E-02	1.518	0.008	2.203E-03	4.098E-05	9.979E-01	1.091E-03	10.001	0.259
^{143}Ce	293.266	7.650E+00	6.745E-02	33.039	0.006	9.562E-03	1.251E-05	9.757E-01	1.226E-02	42.800	0.420

TABLE XIII: Values used to calculate Np2 cumulative fission product yield results and uncertainties for detector 8816 where N_f = 7.5E9 ± 3E8.

Isotope	E_γ (keV)	A_0 (Bq)	ΔA_0 (Bq)	$\tau_{1/2}$ (hrs.)	$\Delta\tau_{1/2}$ (hrs.)	ϵ_γ	$\Delta\epsilon_\gamma$	I_γ	ΔI_γ	R_γ (%)	ΔR_γ (%)
^{88}Kr	196.301	3.012E+01	1.955E-01	2.840	0.030	1.095E-02	9.464E-06	9.450E-01	2.756E-02	25.985	1.214
^{88}Kr	2195.842	2.221E+00	3.456E-02	2.840	0.030	1.994E-03	3.665E-05	9.980E-01	1.046E-03	13.183	0.618
^{88}Kr	2392.110	5.722E+00	3.478E-02	2.840	0.030	1.926E-03	3.936E-05	9.980E-01	1.024E-03	34.600	1.603
^{91}Sr	749.800	5.369E+00	3.957E-02	9.630	0.050	3.702E-03	1.495E-05	9.954E-01	2.341E-03	23.685	0.796
^{92}Sr	1383.930	5.170E+01	1.008E-01	2.710	0.010	2.495E-03	2.465E-05	9.975E-01	1.283E-03	90.000	5.682
^{93}Y	266.900	5.512E+00	1.214E-01	10.180	0.080	8.729E-03	9.694E-06	9.726E-01	1.390E-02	7.320	1.054
^{105}Ru	316.440	7.993E+00	1.103E-01	4.440	0.020	7.540E-03	9.977E-06	9.809E-01	9.731E-03	11.116	0.396
^{105}Ru	393.360	2.602E+00	7.033E-02	4.440	0.020	6.231E-03	1.057E-05	9.876E-01	6.330E-03	3.775	0.062
^{105}Ru	469.370	1.049E+01	8.082E-02	4.440	0.020	5.355E-03	1.133E-05	9.910E-01	4.628E-03	17.548	0.552
^{105}Rh	319.231	1.442E+00	6.351E-02	35.360	0.060	7.482E-03	9.995E-06	9.813E-01	9.555E-03	19.100	0.630
^{127}Sn	1095.600	8.852E-01	1.027E-01	2.100	0.040	2.863E-03	2.018E-05	9.970E-01	1.549E-03	19.380	5.214
^{127}Sn	1114.300	2.114E+00	3.938E-02	2.100	0.040	2.833E-03	2.047E-05	9.970E-01	1.525E-03	38.000	7.965
^{128}Sn	482.300	2.709E+01	1.925E-01	0.984	0.002	5.235E-03	1.147E-05	9.914E-01	4.425E-03	59.000	6.686
^{130}Sb	330.914	1.077E+02	6.291E-01	0.658	0.013	7.250E-03	1.007E-05	9.826E-01	8.873E-03	78.000	4.000
^{130}Sb	793.400	7.510E+01	5.919E-01	0.658	0.013	3.554E-03	1.559E-05	9.957E-01	2.192E-03	100.000	5.000
^{132}Te	228.160	7.747E+00	3.151E-02	76.896	0.312	9.887E-03	9.544E-06	9.608E-01	1.981E-02	88.000	3.478
^{133m}Te	863.955	2.839E+01	2.770E-01	0.923	0.007	3.347E-03	1.664E-05	9.961E-01	1.991E-03	14.887	1.274
^{133m}Te	912.671	9.688E+01	3.654E-01	0.923	0.007	3.224E-03	1.737E-05	9.964E-01	1.874E-03	43.767	3.666
^{133m}Te	1683.230	4.858E+00	8.299E-02	0.923	0.007	2.251E-03	2.921E-05	9.978E-01	1.148E-03	3.945	0.344
^{134}Te	201.235	8.346E+01	5.499E-01	0.697	0.013	1.078E-02	9.472E-06	9.478E-01	2.616E-02	8.850	0.380
^{134}Te	712.970	3.304E+01	5.903E-01	0.697	0.013	3.842E-03	1.443E-05	9.952E-01	2.489E-03	4.720	0.604
^{131}I	364.489	1.355E+00	4.624E-02	192.605	0.014	6.660E-03	1.033E-05	9.857E-01	7.310E-03	81.500	0.759
^{135}I	220.502	3.120E+00	8.437E-02	6.570	0.020	1.014E-02	9.521E-06	9.575E-01	2.141E-02	1.751	0.062
^{135}I	288.451	3.607E+00	5.867E-02	6.570	0.020	8.172E-03	9.807E-06	9.769E-01	1.178E-02	3.100	0.113
^{135}I	1131.511	9.566E+00	5.450E-02	6.570	0.020	2.806E-03	2.074E-05	9.971E-01	1.503E-03	22.587	0.723
^{135}I	1260.409	1.101E+01	5.218E-02	6.570	0.020	2.631E-03	2.274E-05	9.973E-01	1.373E-03	28.700	0.916
^{139}Ba	165.857	1.896E+02	3.222E-01	1.384	0.005	1.189E-02	9.428E-06	9.190E-01	3.999E-02	23.760	0.250
^{142}La	641.285	1.043E+02	2.763E-01	1.518	0.008	4.163E-03	1.344E-05	9.944E-01	2.866E-03	47.400	0.500
^{142}La	894.900	1.415E+01	1.255E-01	1.518	0.008	3.267E-03	1.710E-05	9.963E-01	1.915E-03	8.342	0.167
^{142}La	1043.700	4.315E+00	1.042E-01	1.518	0.008	2.952E-03	1.938E-05	9.968E-01	1.626E-03	2.702	0.055

^{142}La	1233.100	2.680E+00	5.151E-02	1.518	0.008	2.665E-03	2.232E-05	9.973E-01	1.397E-03	1.896	0.051
^{142}La	1901.300	6.384E+00	5.026E-02	1.518	0.008	2.124E-03	3.244E-05	9.979E-01	1.093E-03	7.157	0.161
^{142}La	2055.200	1.779E+00	3.359E-02	1.518	0.008	2.051E-03	3.466E-05	9.979E-01	1.066E-03	2.180	0.098
^{142}La	2100.400	6.945E-01	3.185E-02	1.518	0.008	2.032E-03	3.530E-05	9.979E-01	1.059E-03	1.043	0.095
^{142}La	2187.200	3.519E+00	1.690E+00	1.518	0.008	1.997E-03	3.653E-05	9.980E-01	1.047E-03	3.697	0.103
^{142}La	2542.700	6.097E+00	4.276E-02	1.518	0.008	1.881E-03	4.138E-05	9.980E-01	1.011E-03	10.001	0.259
^{143}Ce	293.266	6.360E+00	6.912E-02	33.039	0.006	8.056E-03	9.833E-06	9.776E-01	1.139E-02	42.800	0.420

VIII. CONCLUSION

The experimental setup and procedure is the same as the previous measurement for ^{235}U , ^{238}U, and ^{239}Pu fission spectrum cumulative fission product yields [27, 29]. The data analysis described can be implemented for any actinide to study fission product γ rays. In this work, 101 γ rays were analyzed for 36 isotopes.

The variations in fission product yield results have been observed in past results [27, 29]. For the case of ^{142}La, the evaluators mainly based the decay scheme from a 1982 measurement [22]. In 1982, a γ-γ coincidence measurement was performed on ^{142}La using Cs fission products of ^{235}U [52]. A shield comprised of 1 mm of Cu, 1 mm of Pb, and 4 mm of B_4C was placed in front of the detectors and an efficiency calibration was performed using ^{152}Eu (with γ-ray branching ratios from 1979 [53]). The attenuation through the detector front shields were not included in the analysis and would cause γ-ray branching ratios to be lower at higher γ-ray energies and vice versa [27].

Similarly to the ^{239}Pu FPY measurement, there are more fission product yield results that exhibit variation for different γ ray analyzed [27]. The similar variation in fission product yield results for different actinides analyzed using the same experimental setup may be caused by discrepancies in γ-ray branching ratios.

IX. FUTURE WORK

^{233}U is the next actinides to have their fission product yields measured using Godiva IV critical assembly. A new experimental setup, called the Lāpaki γ-γ array, was designed and constructed to measure short-lived fission product yield and γ-ray branching ratios [54]. An experiment at Oregon State University will use Lāpaki to measure ^{238}U short-lived fission product yields and fission product γ rays.

ACKNOWLEDGMENTS

This work was funded by the Office of Defense Nuclear Nonproliferation Research and Development within the U.S. Department of Energy's National Nuclear Security Administration by Lawrence Livermore National Laboratory under Contract No DE-AC52-07NA27344. The U.S. Department of Energy's Nuclear Criticality Safety Programs National Criticality Experiments Research Center (NCERC), utilized in this work, is supported by the National Nuclear Security Administration's Office of the Chief of Defense Nuclear Safety, NA-511.

[1] E. McCutchan and A. Sonzogni, "Nuclear data sheets for a = 88," Nucl. Data Sheets **115**, 135 (2014).
[2] C. M. Baglin, "Nuclear data sheets for a = 91," Nucl. Data Sheets **114**, 1293 (2013).
[3] C. M. Baglin, "Nuclear data sheets for a = 92," Nucl. Data Sheets **113**, 2187 (2012).
[4] C. M. Baglin, "Nuclear data sheets for a = 93," Nucl. Data Sheets **112**, 1163 (2011).
[5] S. Basu, G. Mukherjee, and A. Sonzogni, "Nuclear data sheets for a = 95," Nucl. Data Sheets **111**, 2555 (2010).
[6] N. Nica, "Nuclear data sheets for a = 97," Nucl. Data Sheets **111**, 525 (2010).
[7] E. Browne and J. Tuli, "Nuclear data sheets for a=99," Nucl. Data Sheets **145**, 25 (2017).
[8] D. De Frenne, "Nuclear data sheets for a = 103," Nucl. Data Sheets **110**, 2081 (2009).
[9] S. Lalkovski, J. Timar, and Z. Elekes, "Nuclear data sheets for a=105," Nucl. Data Sheets **161-162**, 1 (2019).
[10] A. Hashizume, "Nuclear data sheets for a = 127," Nucl. Data Sheets **112**, 1647 (2011).
[11] Z. Elekes and J. Timar, "Nuclear data sheets for a = 128," Nucl. Data Sheets **129**, 191 (2015).
[12] J. Timar, Z. Elekes, and B. Singh, "Nuclear data sheets for a = 129," Nucl. Data Sheets **121**, 143 (2014).
[13] B. SINGH, "Nuclear data sheets for a = 130," Nucl. Data Sheets **93**, 33 (2001).
[14] Y. Khazov, I. Mitropolsky, and A. Rodionov, "Nuclear data sheets for a = 131," Nucl. Data Sheets **107**, 2715 (2006).
[15] Y. Khazov, A. Rodionov, S. Sakharov, and B. Singh, "Nuclear data sheets for a=132," Nucl. Data Sheets **104**, 497 (2005).
[16] Y. Khazov, A. Rodionov, and F. Kondev, "Nuclear data sheets for a = 133," Nucl. Data Sheets **112**, 855 (2011).
[17] A. Sonzogni, "Nuclear data sheets for a = 134," Nucl. Data Sheets **103**, 1 (2004).

[18] B. Singh, A. A. Rodionov, and Y. L. Khazov, "Nuclear data sheets for a = 135," Nucl. Data Sheets **109**, 517 (2008).
[19] P. K. Joshi, B. Singh, S. Singh, and A. K. Jain, "Nuclear data sheets for a = 139," Nucl. Data Sheets **138**, 1 (2016).
[20] N. Nica, "Nuclear data sheets for a=140," Nucl. Data Sheets **154**, 1 (2018).
[21] N. Nica, "Nuclear data sheets for a = 141," Nucl. Data Sheets **122**, 1 (2014).
[22] T. Johnson, D. Symochko, M. Fadil, and J. Tuli, "Nuclear data sheets for a = 142," Nucl. Data Sheets **112**, 1949 (2011).
[23] E. Browne and J. Tuli, "Nuclear data sheets for a = 143," Nucl. Data Sheets **113**, 715 (2012).
[24] B. Singh, "Nuclear data sheets for a = 151," Nucl. Data Sheets **110**, 1 (2009).
[25] B. D. Pierson, A. M. Prinke, L. R. Greenwood, *et al.*, "Improved cumulative fission yield measurements with fission spectrum neutrons on 235u," Nucl. Data Sheets **155**, 86 (2019).
[26] B. Pierson, L. Greenwood, S. Stave, *et al.*, "Improved cumulative fission yield measurements with fission spectrum neutrons on 238u," Nucl. Data Sheets **163**, 249 (2020).
[27] A. S. Tamashiro, J. T. Harke, S. W. Padgett, *et al.*, "^{239}pu fission spectrum cumulative fission product yield measurement using godiva iv critical assembly." Manuscript submitted (2022).
[28] J. Goda, C. Bravo, T. Cutler, *et al.*, "A new era of nuclear criticality experiments: The first 10 years of godiva iv operations at ncerc," Nucl. Sci. Eng. **195**, S55 (2021).
[29] A. S. Tamashiro, *Evaluation of ^{235}U and ^{238}U Fast Fission Product Yields from Godiva-IV Burst Irradiation via Gamma Detection.* PhD thesis, Oregon State University (2019).
[30] T. England and B. Rider, "Evaluation and compilation of fission product yields 1993," tech. rep., Los Alamos National Lab. (1995).
[31] G. J. Kirouac, H. M. Eiland, and C. J. Slavik, "Fast neutron flux measurement," Tech. Rep. KAPL-P-4005, Knolls Atomic Power Laboratory (1973).
[32] N. D. Dudey, R. J. Popek, R. C. Greenwood, R. G. Helmer, J. W. Rogers, L. S. Kellog, and W. H. Zimmer, "Fission-product-rate measurements and yields," Nucl. Technol. **25**, 294 (1975).
[33] L. S. Kellogg, A. I. Davis, E. P. Lippincott, and J. M. Ruggles, "Edb-ii validated, key fission product yields for fast reactor application," tech. rep., International Atomic Energy Agency, United States (1977). NUREG-CP–0004(Vol3).
[34] A. N. Gudkov, V. M. Zhivun, A. V. Zvonarev, A. F. Zolotov, A. B. Koldobskii, Y. F. Koleganov, V. M. Kolobashkin, S. V. Krivasheev, and N. S. Piven', "Determination of the yield figures of the products resulting from the 237np fission by fast neutrons with the aid of semiconductor spectrometry," Sov. At. Energy (1983).
[35] A. G. C. NAIR, S. K. DAS, B. S. TOMAR, A. GOSWAMI, B. K. SRIVASTAVA, and S. PRAKASH, "Cumulative yields of short-lived ruthenium isotopes in thermal neutron-induced fission of 241pu," Radiochimica Acta **42**, 7 (1987).
[36] A. RAMASWAMI, S. S. RATTAN, N. CHAKRAVARTY, R. J. SINGH, S. B. MANOHAR, S. PRAKASH, and M. V. RAMANIAH, "Charge distribution study in the neutron induced fission of 237np: Fractional cumulative yield of 134te,135i and 138xe," Radiochimica Acta **41**, 9 (1987).
[37] D. Brown *et al.*, "Endf/b-viii.0: The 8th major release of the nuclear reaction data library with cielo-project cross sections, new standards and thermal scattering data," Nucl. Data Sheets **148**, 1 (2018). Special Issue on Nuclear Reaction Data.
[38] B. Singh and J. Chen, "Nuclear data sheets for a=85," Nucl. Data Sheets **116**, 1 (2014).
[39] T. Johnson and W. Kulp, "Nuclear data sheets for a = 87," Nucl. Data Sheets **129**, 1 (2015).
[40] E. Browne and J. Tuli, "Nuclear data sheets for a = 137," Nucl. Data Sheets **108**, 2173 (2007).
[41] J. Chen, "Nuclear data sheets for a=138," Nucl. Data Sheets **146**, 1 (2017).
[42] R. E. Malenfant, "Los alamos critical assemblies facility," tech. rep., Los Alamos Scientific Laboratory (1981).
[43] L. R. Greenwood and C. D. Johnson, "User guide for the staysl pnnl suite of software tools," tech. rep., Pacific Northwest National Lab.(PNNL), Richland, WA (United States) (2013).
[44] R. W. Mills, *Fission Yield evaluation.* PhD thesis, Ph. D. Thesis (1995).
[45] E. Browne and J. Tuli, "Nuclear data sheets for a = 60," Nucl. Data Sheets **114**, 1849 (2013).
[46] M. S. Basunia, "Nuclear data sheets for a = 22," Nucl. Data Sheets **127**, 69 (2015).
[47] Y. Dong and H. Junde, "Nuclear data sheets for a = 54," Nucl. Data Sheets **121**, 1 (2014).
[48] M. Berger, J. Hubbell, S. Seltzer, J. Chang, J. Coursey, R. Sukumar, D. Zucker, and K. Olsen, "*XCOM: Photon Cross Section Database* (version 1.5)," NIST **[Online] Available: http://physics.nist.gov/xcom [2020, February 27]. National Institute of Standards and Technology, Gaithersburg, MD.** (2020).
[49] M. J. Berger, J. Coursey, M. Zucker, , J. Chang, *et al.*, *Stopping-power and range tables for electrons, protons, and helium ions.* NIST Physics Laboratory Gaithersburg, MD (1998).
[50] R. Brun and F. Rademakers, "Root—an object oriented data analysis framework," Nucl. Inst. Meth. Phys. Res. Sect. A: Accel. Spectrometers, Detect. Assoc. Equip. **389**, 81 (1997).
[51] G. F. Knoll, *Radiation Detection and Measurement.* Wiley (2010).
[52] E. Michelakakis, W. D. Hamilton, P. Hungerford, G. Jung, P. Pfeiffer, and S. M. Scott, "Levels and transitions in^{142,144}ce populated following the β decay of^{142,144}la," J. Phys. G: Nucl. Phys. **8**, 111 (1982).
[53] K. Debertin, "International intercomparison of gamma-ray emission-rate measurements by means of germanium spectrometers and 152eu sources," Nucl. Inst. Meth. **158**, 479 (1979).
[54] A. S. Tamashiro, J. T. Harke, J. G. Duarte, *et al.*, "The lāpaki γ-γ array." Manuscript submitted (2022).